THE JOURNAL OF COMPARATIVE NEUROLOGY 366:613–642 (1996)

Auditory Pathways of Caudal Telencephalon and Their Relation to the Song System of Adult Male Zebra Finches (*Taenopygia guttata*)

G. EDWARD VATES, BEDE M. BROOME, CLAUDIO V. MELLO, AND FERNANDO NOTTEBOHM
Laboratory of Animal Behavior, The Rockefeller University, New York, New York 10021

ABSTRACT

Auditory information is critical for vocal imitation and other elements of social life in songbirds. In zebra finches, neural centers that are necessary for the acquisition and production of learned vocalizations are known, and they all respond to acoustic stimulation. However, the circuits by which conspecific auditory signals are perceived, processed, and stored in long-term memory have not been well documented. In particular, no evidence exists of direct connections between auditory and vocal motor pathways, and two newly identified centers for auditory processing, caudomedial neostriatum (Ncm) and caudomedial hyperstriatum ventrale (cmHV), have no documented place among known auditory circuits. Our goal was to describe anatomically the auditory pathways in adult zebra finch males and, specifically, to show the projections by which Ncm and vocal motor centers may receive auditory input. By using injections of different kinds of neuroanatomical tracers (biotinylated dextran amines, rhodamine-linked dextran amines, biocytin, fluorogold, and rhodamine-linked latex beads), we have shown that, as in other avian groups, the neostriatal field L complex in caudal telencephalon is the primary forebrain relay for pathways originating in the auditory thalamus, i.e., the nucleus ovoidalis complex (Ov). In addition, Ncm and cmHV also receive input from the Ov complex. Ov has been broken down into two parts, the Ov "core" and "shell," which project in parallel to different targets in the caudal telencephalon. Parts of the field L complex are connected among themselves and to Ncm, cmHV, and caudolateral HV (clHV) through a complex web of largely reciprocal pathways. In addition, clHV and parts of the field L complex project strongly to the "shelf" of neostriatum underneath the song control nucleus high vocal center (HVC) and to the "cup" of archistriatum rostrodorsal to another song-control nucleus, the robust nucleus of the archistriatum (RA). We have documented two points at which the vocal motor pathway may pick up auditory signals: the HVC-shelf interface and a projection from clHV to the nucleus interfacialis (NIf), which projects to HVC. These data represent the most complete survey to date of auditory pathways in the adult male zebra finch brain, and of their projections to motor stations of the song system.

Indexing terms: HVC, Ncm, shelf, field L complex, birdsong

Auditory information plays an important role in the social and reproductive biology of oscine songbirds (order Passeriformes) and is necessary for many tasks, including vocal imitation (Thorpe, 1958; Marler and Tamura, 1964; Konishi, 1965; Nottebohm, 1968; Marler and Peters, 1977, 1981, 1982), territorial defense (Peek, 1972; Krebs, 1977), courtship (Kroodsma, 1976), offspring and neighbor recognition (Weeden and Falls, 1959; Brooks and Falls, 1975; Wiley and Wiley, 1977; Falls, 1982; Beecher et al., 1986; Godard, 1991), countersinging (Hinde, 1958; Falls et al., 1982, 1988), and antiphonal duetting (Thorpe, 1963; Thorpe and North, 1965; Brenowitz and Arnold, 1989). Vocal imitation plays an especially important role in the vocal ontogeny of perhaps all songbirds (Nottebohm, 1972; Kroodsma, 1982). It requires that individuals remember the song and calls of other birds (usually those of the same species) and use these memories as models to guide vocal

Accepted December 7, 1995.

Address reprint requests to G. Edward Vates, Laboratory of Animal Behavior, The Rockefeller University, 1230 York Avenue, Box 137, New York, NY 10021. Email: vatese@rockvax.ROCKEFELLER.EDU.

development. Vocal learning with reference to an adult model has been amply documented in juvenile zebra finches (*Taenopygia guttata*; Immelman, 1969; Price, 1979; Zann, 1985; Williams, 1990). This dependence on auditory information persists in adulthood, because deafening after song crystallization is often followed by the gradual decay of the song that had been mastered (Nordeen and Nordeen, 1992). In addition, the processing of auditory information by song circuits could play a role in the perception of conspecific sounds (Williams and Nottebohm, 1985; Brenowitz, 1991).

Thus, there are at least two reasons why auditory information should reach brain pathways involved in vocalization: 1) for learning and maintenance of vocalizations and 2) for guiding and perhaps interpreting vocal exchanges. Despite these expectations, there is as yet no clear picture of the projections between auditory and vocal pathways that might guide vocal exchanges and the acquisition and maintenance of learned song.

The neural pathways responsible for the acquisition and production of learned vocalizations in songbirds consist of discrete nuclei and projections. The main motor pathway goes from the high vocal center (HVC) to the robust nucleus of the archistriatum (RA), which in turn innervates mesencephalic and medullary nuclei involved in vocalization (Nottebohm et al., 1976, 1982; McCasland and Konishi, 1981; Simpson and Vicario, 1990; Vicario and Nottebohm, 1990; Vicario, 1991, 1993; Wild, 1993, 1994). Other telencephalic and thalamic nuclei necessary for song acquisition but not for song production have been identified, and their anatomy and physiology have been extensively studied (Bottjer et al., 1984, 1989; Sohrabji et al., 1990; Scharff and Nottebohm, 1991; Okuhata and Saito, 1987; Williams, 1989; Okuhata and Nottebohm, 1992; Johnson et al., 1995; Vates and Nottebohm, 1995). Electrophysiological recordings have shown that all of the nuclei mentioned above respond to auditory stimuli (Katz and Gurney, 1981; McCasland and Konishi, 1981; Williams, 1989) and that, in adults, they respond maximally to the bird's own song (Margoliash, 1983, 1986; Doupe and Konishi, 1991; Vicario and Yohay, 1993). Clearly, then, song motor pathways receive input from auditory processing pathways.

A large number of studies have detailed how auditory information travels in the avian brain from the cochlear nuclei to the thalamic auditory relay nucleus ovoidalis (Ov) and from there to the telencephalic field L complex (Karten, 1967, 1968; Kelley and Nottebohm, 1979; Brauth et al., 1987, 1994; Wild, 1987; Durand et al., 1992; Wild et al., 1993). The field L complex in oscines and nonoscines projects to many other areas in the telencephalon, creating a widely branching network of pathways in adjacent neostriatum, caudal hyperstriatum ventrale, and archistriatum (Bonke et al., 1979a; Kelley and Nottebohm, 1979; Saini and Leppelsack, 1981; Brauth and McHale, 1988; Fortune and Margoliash, 1992; Wild et al., 1993; Brauth et al., 1994); together, some or all of these areas have been likened to an avian homologue of the mammalian auditory cortex (Bonke et al., 1979b; Scheich et al., 1979; Müller and Leppelsack, 1985; Müller and Scheich, 1985; Brauth and McHale, 1988; Scheich, 1990; Heil and Scheich, 1991a,b; Wild et al., 1993; Brauth et al., 1994).

Many of these studies, however, have been carried out in nonsongbird species [e.g., ring doves (*Streptopelia risoria*), pigeons (*Columba livia*), Guinea fowl (*Numida meleagris*), and budgerigars (*Melopsittacus undulatus*)], and those in songbirds have not yet shown any convincing pathways by which auditory information may be transmitted to the song control circuits. Early work by Kelley and Nottebohm (1979) in canary (*Serinus canaria*) failed to demonstrate a direct source of auditory input to vocal motor centers, although they did show that field L projects to a layer of tissue ventral and medial to HVC referred to as the "shelf," as well as to a "cup" of tissue anteroventral to RA. Attempts to determine whether the HVC shelf or perhaps field L project into HVC have been equivocal (Katz and Gurney, 1981; Margoliash, 1987; Fortune and Margoliash, 1995). HVC has three known inputs: the medial magnocellular nucleus of the anterior neostriatum (mMAN), the nucleus uvaeformis of the thalamus (Uva), and the nucleus interfacialis of caudal neostriatum (NIf; Nottebohm et al., 1982). Uva and NIf respond to auditory stimuli, but their connections to auditory centers remain undefined (Williams, 1989; Okuhata and Nottebohm, 1992); there is no report of auditory responses in mMAN.

Our interest in the relation between auditory and vocal circuits was rekindled recently by the identification of new potential centers for auditory processing. ZENK, a transcrip-

*Abbreviations**

A	archistriatum
APH	parahippocampal area
BDA	biotinylated dextran amines
ChO	optic chiasm
cHV	caudal hyperstriatum ventrale
clHV	caudolateral hyperstriatum ventrale
cmHV	caudomedial hyperstriatum ventrale
DLM	medial nucleus of the dorsolateral thalamus
Flg	Fluorogold
FPL	lateral forebrain bundle (fasciculus prosencephalus lateralis)
HP	hippocampus
HVC	high vocal center
L, L1, L2a, L2b, L3	cytoarchitectonic subdivisions of the neostriatal field L complex in caudal telencephalon
LAD	dorsal archistriatal lamina
LH	lamina hyperstriatica
LL	lateral lemniscus
lMAN	lateral magnocellular nucleus of the anterior neostriatum
LMD	lamina medularis dorsalis
MLd	dorsal part of the lateral mesencephalic nucleus
mMAN	medial magnocellular nucleus of the anterior neostriatum
Nc	caudal neostriatum
Ncm	caudomedial neostriatum
NI	intermediate neostriatum
NIf	nucleus interfacialis
Ov	nucleus ovoidalis
Ovm	medial part of nucleus ovoidalis
PA	paleostriatum augmentatum
Paleo	paleostriatum
PP	paleostriatum primitivum
RA	robust nucleus of the archistriatum
RDA	tetramethylrhodamine-linked dextran amines
SPO	nucleus semilunaris parovoidalis
tOM	tractus occipitomesencephalicus
tOv	tractus ovoidalis
Uva	nucleus uvaeformis of the thalamus
X	area X of the parolfactory lobe

*Note that anatomical qualifiers, such as "caudal" and "medial," are ordinarily abbreviated as small letters that follow capitalized letters signifying the qualified anatomical location (e.g., caudomedial neostriatum is abbreviated as Ncm). In this paper, we have chosen to abbreviate caudolateral hyperstriatum ventrale as clHV and caudomedial hyperstriatum ventrale as cmHV to avoid confusion with the abbreviation for the high vocal center, HVC, which was previously named incorrectly as hyperstriatum ventrale pars caudale (HVc).

tional regulator that is highly sensitive to membrane depolarization, is rapidly induced in the songbird brain in response to conspecific song playbacks (Mello et al., 1992). In particular, ZENK expression is induced by conspecific song in the caudomedial neostriatum (Ncm), a region previously unrecognized as an auditory center, as well as in other previously identified parts of the auditory circuit, such as the caudomedial hyperstriatum ventrale (cmHV; Mello et al., 1992; Mello and Clayton, 1994). The results of these gene-induction experiments as well as recent investigations into the physiological response of Ncm to song playbacks (Chew et al., 1995a,b) suggest that Ncm and cmHV may play a critical role in auditory perception, discrimination, and even formation of auditory memories. Although evidence exists for auditory inputs from the field L complex into caudal HV (cHV; Bonke et al., 1979a; Saini and Leppelsack, 1981), there are no descriptions of the anatomical connections of Ncm. Consequently, we were especially interested in determining whether Ncm and cmHV received auditory projections that might account for the activation of ZENK expression there following song presentation and whether Ncm or cmHV sent projections that could influence the pathways that control singing behavior.

We placed injections of different kinds of anterograde and retrograde neuroanatomical tracers into known thalamic and telencephalic auditory relay centers in order to trace the course of presumed auditory connections from these areas to other auditory stations described in previous anatomical and gene expression studies. Our goal was to provide as complete a description as possible of auditory processing pathways and, specifically, the pathways by which Ncm and the vocal motor pathway receive auditory input.

MATERIALS AND METHODS

Experiments were conducted with a total of 70 adult male zebra finches (*Taenopygia guttata*; >120 days old) that were obtained from our own breeding colonies at the Rockefeller University Field Research Center (Millbrook, NY).

Injections of neuronal tract tracers

For all surgery, anesthesia was induced with Nembutal (50 mg/kg body weight) and was maintained with Metofane inhalation as needed. Each bird was placed in a stereotaxic apparatus, and the skin over the skull was opened. Small windows in the skull were opened over desired targets. All targets were injected by using glass micropipettes (10–25 μm o.d.) at previously determined stereotaxic coordinates based on modifications of a canary atlas (Stokes et al., 1974). For certain targets, the penetration was angled to avoid leakage of tracer through areas of interest. For injections into Ov, the target was identified before injection by using microelectrode recordings of neuronal responses to an auditory stimulus, as described previously (Cynx et al., 1992).

Anterograde tracing. Either biotinylated dextran amine [BDA; 10% in phosphate-buffered saline (PBS); 3,000 MW; Molecular Probes, Eugene, OR] or biocytin (5% in 2 M sodium methyl sulfate; Sigma, St. Louis, MO) was injected iontophoretically with a Midgard current source (3–5 μA; 7 seconds on/off; 10–30 minutes).

Retrograde tracing. Fluorogold (FLG; 2% in saline) or rhodamine-linked latex microspheres (beads; Lumafluor) were pressure injected (10–20 nl) by using a hydraulic microinjection system that was developed in our laboratory. BDA or tetramethylrhodamine-linked dextran amine (RDA; 10% in PBS; 3,000 MW; Molecular Probes) were also used as retrograde tracers where targets required the precision of small iontophoretic injections.

Following survival times ranging from 24 hours (biocytin) to 4–8 days (BDA, RDA, FLG, and beads), birds were killed under deep Nembutal anesthesia. Fixation was by intracardiac perfusion with 10 ml of saline followed either by 4% paraformaldehyde (PFA) in 0.1 M phosphate buffer (PB), pH 7.4, for BDA, RDA, FLG, and beads or by 4% PFA/0.05% glutaraldehyde in PB for biocytin.

Histology

For brains injected with BDA or biocytin, each brain hemisphere was cut serially into 50 μm sagittal sections on a Vibratome (Lancer) and collected in PBS. Every other section was then reacted to visualize BDA or biocytin by first incubating in 5% skim milk, 0.3% Triton X-100 in PBS followed by avidin-biotin complex solution (ABC; Vectastain Elite Kit; Vector Laboratories, Burlingame, CA). After several rinses in PBS, BDA- or biocytin-filled cells were revealed by incubation in 0.03% 3,3′-diaminobenzidine (DAB), 0.15% nickel-ammonium sulfate, 0.001% H_2O_2 in PBS. Sections were subsequently rinsed in PBS, mounted onto chromalum slides, air dried overnight, delipidized in xylene, and coverslipped with Krystalon. Alternate sections were not reacted in ABC/DAB but, instead, were mounted immediately and counterstained with 0.5% cresyl violet acetate.

For brains injected with fluorescent tracers, each brain hemisphere was soaked in increasing concentrations of sucrose in 4% PFA until equilibrated in 30% sucrose in 4% PFA. Each hemisphere was then cut serially into 50 μm sagittal sections on the freezing stage of a sliding microtome (American Optical) and collected in PBS. Each section was then mounted onto chromalum-coated slides, air dried overnight in the dark, delipidized briefly by dipping in xylene, and coverslipped with Krystalon.

Sections were viewed with both light and darkfield optics. Projections were traced by using a camera lucida system or a computer-yoked microscope (Alvarez-Buylla and Vicario, 1988).

RESULTS

Figure 1 provides an introduction to the zebra finch telencephalic areas that are discussed in this paper. Field L, as initially described by Rose (1914) in chicken, consisted of a region in the caudomedial neostriatum of birds characterized by small, densely packed, darkly stained neurons. Karten (1968) showed that this brain region in pigeons was the primary recipient of axons from the thalamic auditory relay nucleus Ov. The most recent description of the cytoarchitecture of field L in zebra finches (Fortune and Margoliash, 1992) provides the nomenclature that we have used. This report divided the field L complex into five cytoarchitectonic subdivisions, based on Nissl and Golgi observations: L1, L2a, L2b, L3, and L. The locations of these regions as well as song-control nuclei HVC and NIf are shown schematically and in corresponding Nissl-stained parasagittal and frontal sections in Figure 1. These particular planes of section were chosen because they are representative of the planes of section used in most of the

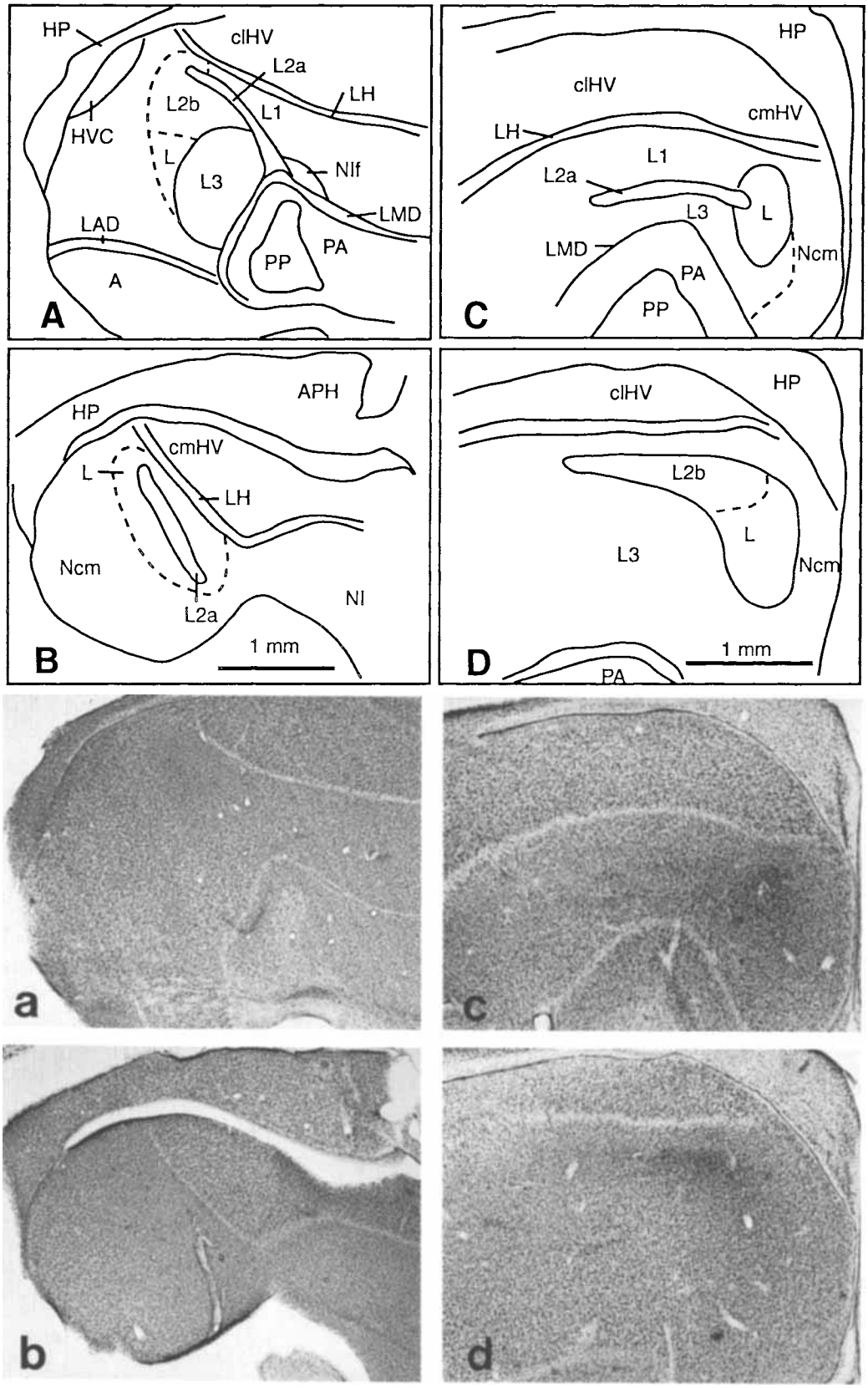

Fig. 1. Outline drawings of parasagittal sections (**A,B**) and frontal sections (**C,D**) of zebra finch brain showing major components of the auditory telencephalon. A is lateral to B, and, for both A and B, dorsal is up and anterior is to the right. C is rostral to D, and, for both, dorsal is up and medial is to the right. Corresponding photomicrographs of Nissl-stained sections are shown below (**a–d**). Solid lines mark the borders of well-defined regions in Nissl-stained sections under microscopic examination (e.g., field L2a of the neostriatal field L complex in caudal telencephalon). Dashed lines mark borders that, in our hands, were more difficult to establish in Nissl-stained sections (e.g., field L2b) and are included to provide approximations of where these different areas are located based on the work of Fortune and Margoliash (1992), which provides a more complete description of how these areas were delineated (after Fortune and Margoliash, 1992). For abbreviations, see list.

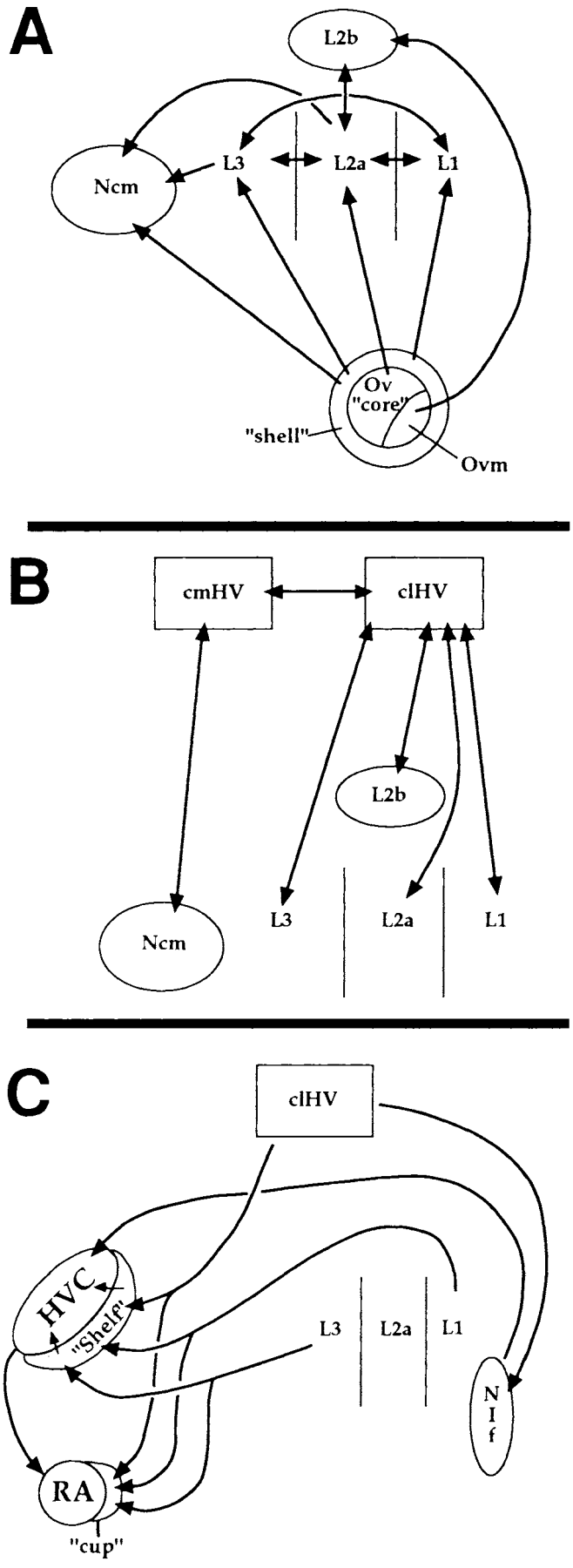

following figures. Some of the identified regions, such as Ncm and cmHV, lack clear lateral borders, and these lateral borders have been defined operationally by their distance from the midline. We will show later in this report that anatomical studies have provided evidence for the discrete nature of these areas.

Figure 2 is a schematic representation of the major findings in this paper. It has been organized into three sections that roughly correspond to three different hierarchical levels of connectivity within the caudal telencephalon. The first part (Fig. 2A) depicts thalamic inputs to auditory telencephalon and the interconnections of thalamorecipient neostriatum. The second part (Fig. 2B) summarizes the connections between thalamorecipient neostriatum and overlying cHV. The third part (Fig. 2C) depicts projections from thalamorecipient neostriatum and cHV to auditory centers adjacent to song nuclei as well as projections to song nuclei themselves. In the following sections of this report, we have described the inputs and outputs of each of the areas identified in this figure. The reader should use this figure as a "touchstone" for placing the detailed anatomy to be described below in a broader context. Table 1 provides a summary of the birds used in this report, detailing the target of injection and the tracer used. In most cases, each bird received an injection into both brain hemispheres but usually into different targets from side to side. For targets for which there was a question of interhemispheric connections, unilateral injections were made, as indicated in Table 1.

Inputs to fields L2a and L2b

Thalamic input to the field L complex. Injections of anterograde tracers into Ov demonstrated a strong projection from Ov to parts of the field L complex (Fig. 3). These injections, which were large and included Ov as well as part of the auditory input fiber pathway tractus ovoidalis (tOv; Fig. 3D–G), labeled fibers that streamed dorsally through the thalamus in the lateral forebrain bundle [fasciculus prosencephalus lateralis (FPL)]. Fibers entered the telencephalon by passing under and through the tractus occipitomesencephalicus (tOM), through the caudal paleostriatum primitivum (PP) and augmentatum (PA), and continued to course dorsally. In sagittal sections, the vast majority of these fibers were seen to terminate in regions that corresponded to the Nissl-stained borders of fields L2a and L2b. In particular, labeled fibers rose through the paleostriatum, crossed the lamina medularis dorsalis (LMD), and formed terminal fields that covered the fiber-rich plate of tissue, which extended in a dorsocaudal direction from the dorsal bend of LMD to a point just ventral to lamina hyperstriatica (LH; i.e., L2a); in addition, terminal fields were observed dorsocaudal to the dorsal tip of L2a, covering the area of densely packed neurons characteristic of L2b. Much more sparse terminations were observed over regions that flanked field L2a rostrally and caudally, i.e., subdivisions L1 and L3 respectively. Smooth fibers were observed in paleostriatum, but it was difficult to determine whether these were fibers passing through paleostriatum on their way to the field L complex or were actually forming synapses in paleostriatum, as has been suggested in Guinea fowl (Bonke et al.,

Fig. 2. **A–C:** A series of schematic representations of the connections discussed in this report. A detailed description is provided in the text. Note that projections to paleostriatum are not included here. For abbreviations, see list.

TABLE 1. Catalog of Brain Hemispheres Injected in a Particular Target and Tracers Used[1]

Tracer	Targeted area												Neostriatum under "shelf"
	Ov	L2a	L2b	L1	L3	clHV	cmHV	Ncm	Shelf	Cup	HVC	NIf	
BDA	3***	3*	4	6*	3*	6	7*	6*	4**	2	5*	2*	4
Biocytin		1	1	3*	2	4	6	6	5				
FLG				1	2			2			1		
Beads		2*	1	4*	5*	2	2	3*	3*	2*	3*	1	
RDA											2	1	

[1]Each number represents the number of brain hemispheres injected at the indicated target for that column with the tracer for that row. In most cases, both hemispheres were injected in one bird but usually in a different area in each hemisphere. For targets where there was a possibility of contralateral projections, unilateral injections were placed; they are indicated by asterisks, with the number of asterisks corresponding to the number of brains injected in one hemisphere only. Total number of subjects used = 70 adult male zebra finches. For abbreviations, see list.

1979a) and canaries (Kelley and Nottebohm, 1979) and has been confirmed in pigeons (Wild et al., 1993) and ring doves (Durand et al., 1992). Injections into Ov also labeled fibers in a portion of neostriatum caudal to medial L2a (Fig. 3G), including an area marked by Fortune and Margoliash (1992) as field L, but with fibers extending beyond into anatomically unstudied Ncm (Mello et al., 1992; Mello and Clayton, 1994; Chew et al., 1995a,b). It is important to note that these fibers did not completely cover Ncm but, instead, left a caudal region of Ncm free of innervation from Ov. We could not distinguish any cytoarchitectonic borders in Nissl-stained sections that correlated with this boundary. Apparently, then, the projection from Ov to Ncm defined two different regions within Ncm that were not immediately obvious in Nissl-stained material but that could be distinguished by the presence or absence of innervation from Ov. This difference in Ov innervation of anterior and posterior Ncm has not been confirmed retrogradely, although the presence of an input to Ncm from Ov has been confirmed (see below). In addition, our anterograde injections into Ov may not have included all parts of the Ov complex that project to Ncm, thus giving an incomplete picture of the projections from Ov to Ncm.

In Nissl-stained sections, Ov can be broken down into a "core" and a "shell" (Fig. 4). The Ov core consists of a number of neuronal clusters that differ on the basis of cell size, Nissl-staining intensity, and packing density. This core is surrounded by the fibrous capsule, or shell, which itself contains smaller, fusiform neuronal cell bodies whose long axes are oriented along the circumference of Ov. The shell merges ventrally with the Ov input pathway, the tOv. Injections of retrograde tracers into the field L complex confirmed that both Ov core and Ov shell project to parts of the field L complex. When our injections were limited to field L2a, retrogradely filled cells were only found within the Ov core (Fig. 5A,a1–3). In contrast, injections of retrograde tracers targeted to fields L1, L3, or Ncm backfilled neurons predominantly in the periphery of the Ov core and in tOv (Fig. 5B,b1–3). Comparing the backfills from fields L1, L3, or Ncm to cresyl-stained alternate sections, we found that the backfilled neurons were in a shell of cells limited to the periphery of Ov, overlapping with the myelinated fiber capsule of Ov and with tOv, but also extending inward to include some cells in the outer one-third of the Ov core.

Injections of retrograde tracers centered on the dorsal edge of L2a labeled cells in the ventral half of Ov core, whereas injections into the ventral part of L2a backfilled cells in the dorsal half of Ov (Fig. 6). Injections into the lateral half of field L2a labeled cells in the lateral extent of Ov core, whereas injections into the most medial part of L2a backfilled cells in the medial portion of Ov core (not shown). Thus, the projection from Ov core to field L2a is topographic, in accordance with observations in starlings, pigeons, and budgerigars (Hauesler, 1988; Wild et al., 1993; Brauth et al., 1994). This topography is inverted along the dorsoventral axis but not along the mediolateral axis. We observed no obvious topography in the projection from Ov shell to fields L1 and L3 or to Ncm.

Injections of retrograde tracers into field L2b labeled a specific subset of neurons in the Ov core that were located at the ventromedial aspect of the nucleus (Fig. 7). We assume that our injections into field L2b did not encroach on L2a, because the cells that were backfilled within Ov were localized to a portion of the Ov core that was not only ventral (as expected) but was also medial; injections into field L2a at similar distances from the midline backfilled cells in more lateral Ov core. When carefully examined, the collection of backfilled neurons in ventromedial Ov was limited to a discrete part of the Ov core that, in Nissl-stained sections, was distinguished by the larger cell diameters of its neurons (Fig. 7B). In a preliminary report, Fortune and Margoliash (1991) reported that field L2b received a specific input from an area adjacent to Ov that they called nucleus ovoidalis medialis (Ovm). Although we could not conclude that the region containing labeled neurons after injections into L2b was separate from Ov core, we believe it represents a part of the Ov complex that specifically projects to L2b; therefore, we call it Ovm, using the nomenclature of Fortune and Margoliash (1991).

Injections of BDA into Ov also backfilled two interesting collections of cells rostral and caudal to Ov that have not been described previously (Fig. 3F). It is important to note that the adjacent thalamic cells backfilled from Ov were not part of the Ov shell, which is closely apposed to the Ov core. We also observed a scattered population of backfilled cells within tOM where it passes rostral to Ov (Fig. 3E). We do not know the function of these areas or their relation to auditory processing in Ov, and we have not used anterograde tracers to confirm their projections to Ov. Backfilled cells were also observed in the dorsal part of the lateral mesencephalic nucleus (MLd) and portions of the lateral lemniscus, as expected from previous studies of ascending

Fig. 3. **A–G:** A lateral-to-medial series of camera lucida drawings of parasagittal sections through the telencephalon showing the ascending projections into the field L complex resulting from an injection of biotinylated dextran amines (BDA) into nucleus ovoidalis (Ov; marked in black). Large black dots represent backfilled cells, short black lines represent labeled fibers, and stippling shows terminations, with the density of stippling roughly corresponding to the density of labeled terminals. The interval between sections is 300 μm, with G ~ 400 μm from the midline. For abbreviations, see list.

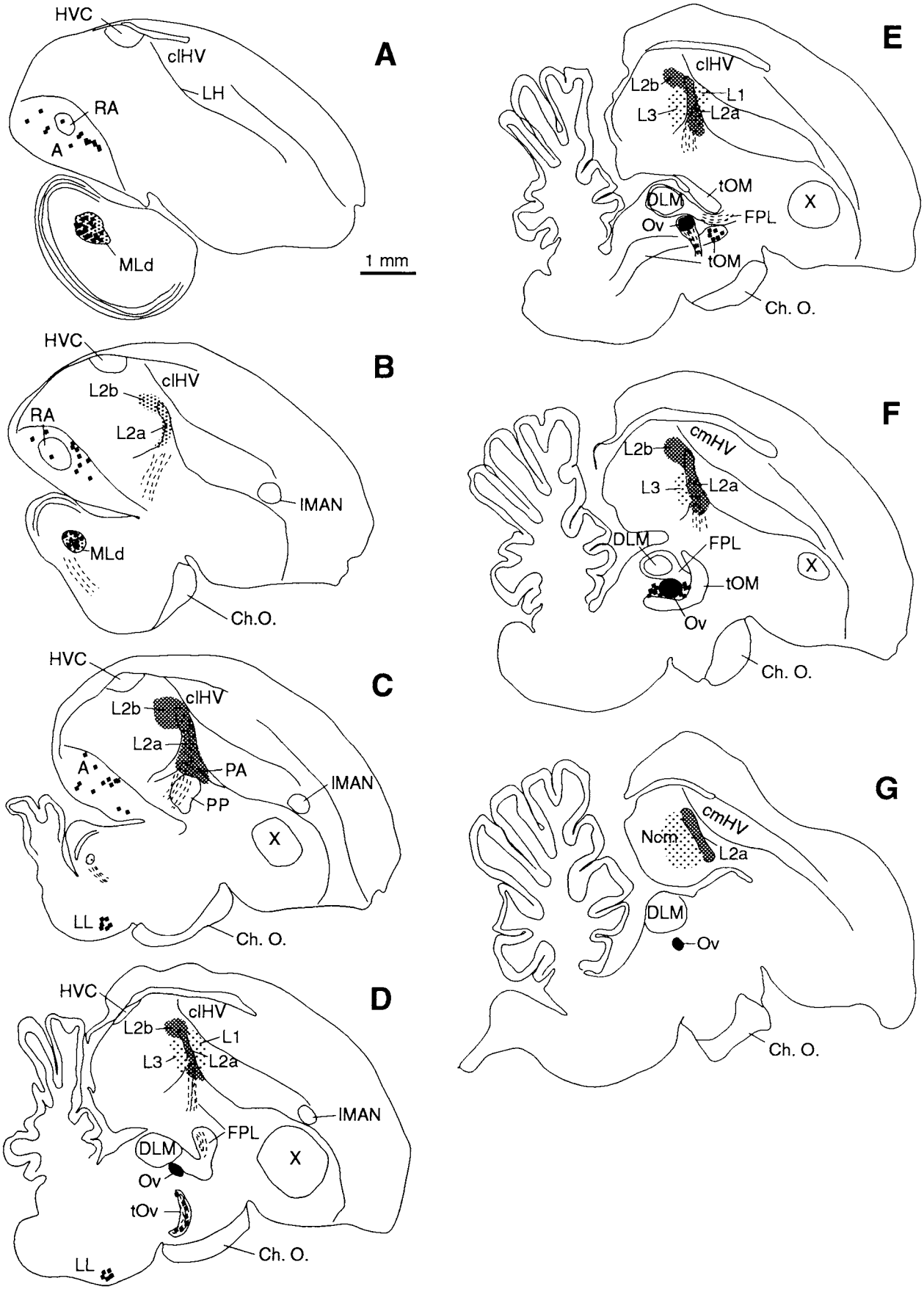
A
HVC
clHV
LH
RA
A
MLd
1 mm
B
HVC
clHV
L2b
RA
L2a
IMAN
MLd
Ch.O.
C
HVC
clHV
L2b
L2a
A
PA
PP
IMAN
X
LL
Ch. O.
D
HVC
clHV
L2b
L1
L3
L2a
IMAN
FPL
DLM
Ov
X
tOv
LL
Ch. O.
E
clHV
L2b
L1
L3
L2a
tOM
DLM
FPL
Ov
X
tOM
Ch. O.
F
cmHV
L2b
L3
L2a
DLM
FPL
tOM
X
Ov
Ch. O.
G
cmHV
Nom
L2a
DLM
Ov
Ch. O.

Figure 3

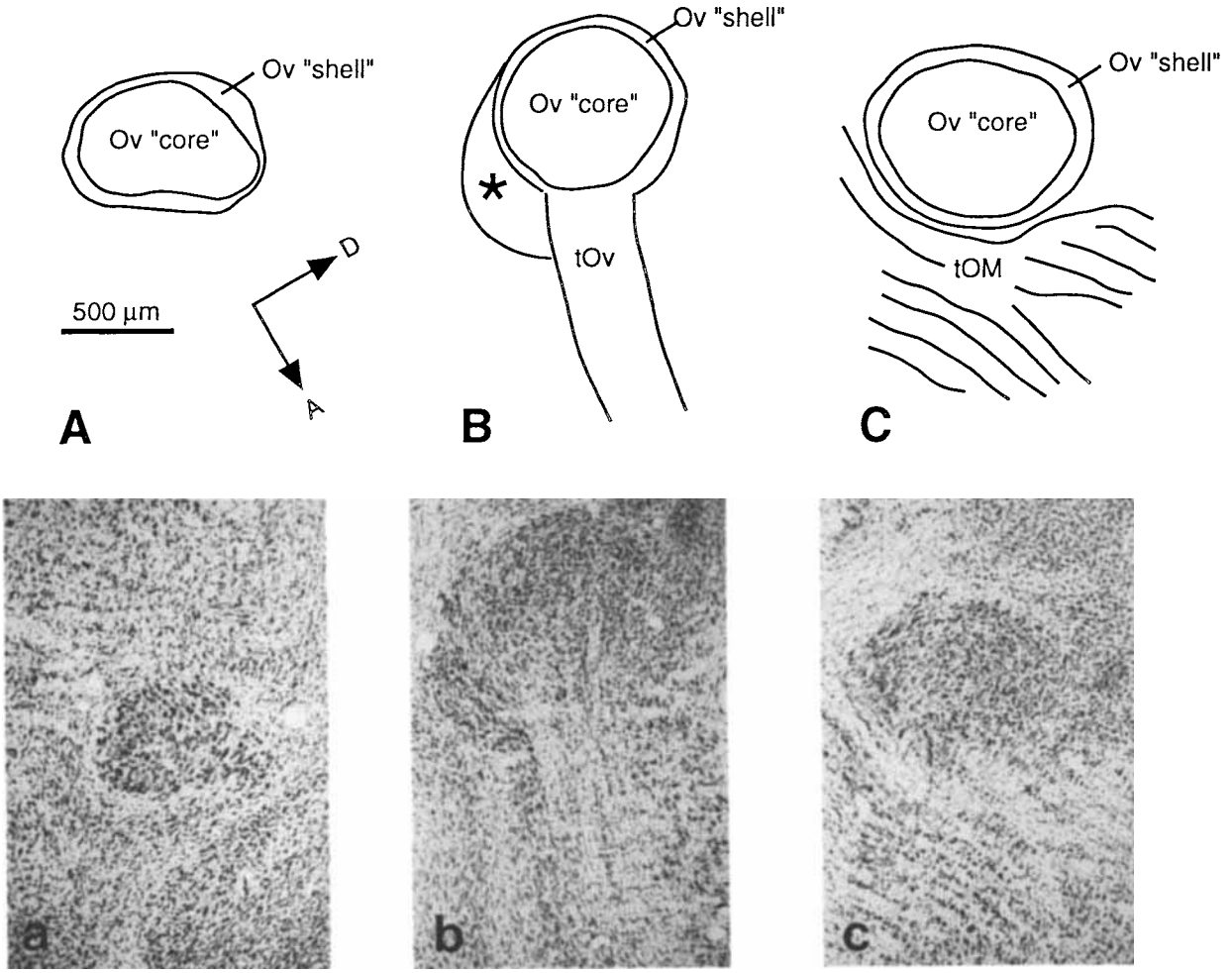

Fig. 4. A lateral-to-medial series of camera lucida drawings of parasagittal sections (**A–C**) through the ovoidalis complex with corresponding photomicrographs of Nissl-stained sections shown below (**a–c**). The area marked with an asterisk (B) is not included as part of the Ov complex, because it lies outside of the fiber-rich "shell," and it never contained retrogradely labeled cells after injection of tracers into the field L complex. For abbreviations, see list.

auditory pathways to the thalamus (Karten, 1967; Wild, 1987). Also, a number of backfilled cells were observed in the archistriatum near RA; a future report will describe the projections from archistriatum to auditory thalamus in more detail (Mello and Vates, unpublished observations).

Telencephalic inputs to fields L2a and L2b. Our injections also showed that both field L2a and L2b receive projections from fields L1, L3, and cHV. Because these connections are reciprocal, they will be discussed in more detail below.

Efferent projections of field L2a

Figure 8 shows an example of a BDA injection limited to lateral field L2a. It was made at a 9° posterior angle to avoid passing through cHV and field L1. Interestingly iontophoretically injected tracers, such as BDA and biocytin, had a remarkable tendency in our hands to respect cytoarchitectonic borders defined by arrays of myelinated fibers. Consequently, iontophoretic injections into or around L2a tended to remain either in or out of L2a, respectively. Injections into L2a (BDA and biocytin) labeled many axons in neighboring regions of auditory neostriatum (fields L1, L2b, and L3) as well as in parts of cHV immediately dorsal to the field L complex (Fig. 8C). To distinguish the part of cHV dorsal to field L from the part of cHV anterodorsal to Ncm, we have called these two regions caudolateral HV (clHV) and caudomedial HV (cmHV) respectively. It is important to note that cHV extends far lateral to the field L complex, and that consequently what we have identified as clHV is not the lateralmost extension of cHV. However, cHV lateral to the part we have studied has not been examined anatomically or functionally, to our knowledge, and for the purposes of clarity and organization, we have designated the parts of cHV under discussion in this report as the cmHV and clHV tiers, with the understanding that this nomenclature may change with expanding knowledge of other parts of cHV. Within fields L1, L2b and L3, the processes from L2a formed dense networks of fibers with numerous varicosities. Because our injection tracts usually passed through L2b in order to reach L2a, we could not rule out the possibility of leakage of tracers directly into L2b. However, we have controlled for this possibility by injecting retro-

grade tracers into field L2b (see below). In addition, injections into lateral L2a resulted in labeling of projection fibers which ramified far medially in L2b, suggesting a true projection from L2a to L2b. In field L1, some of the

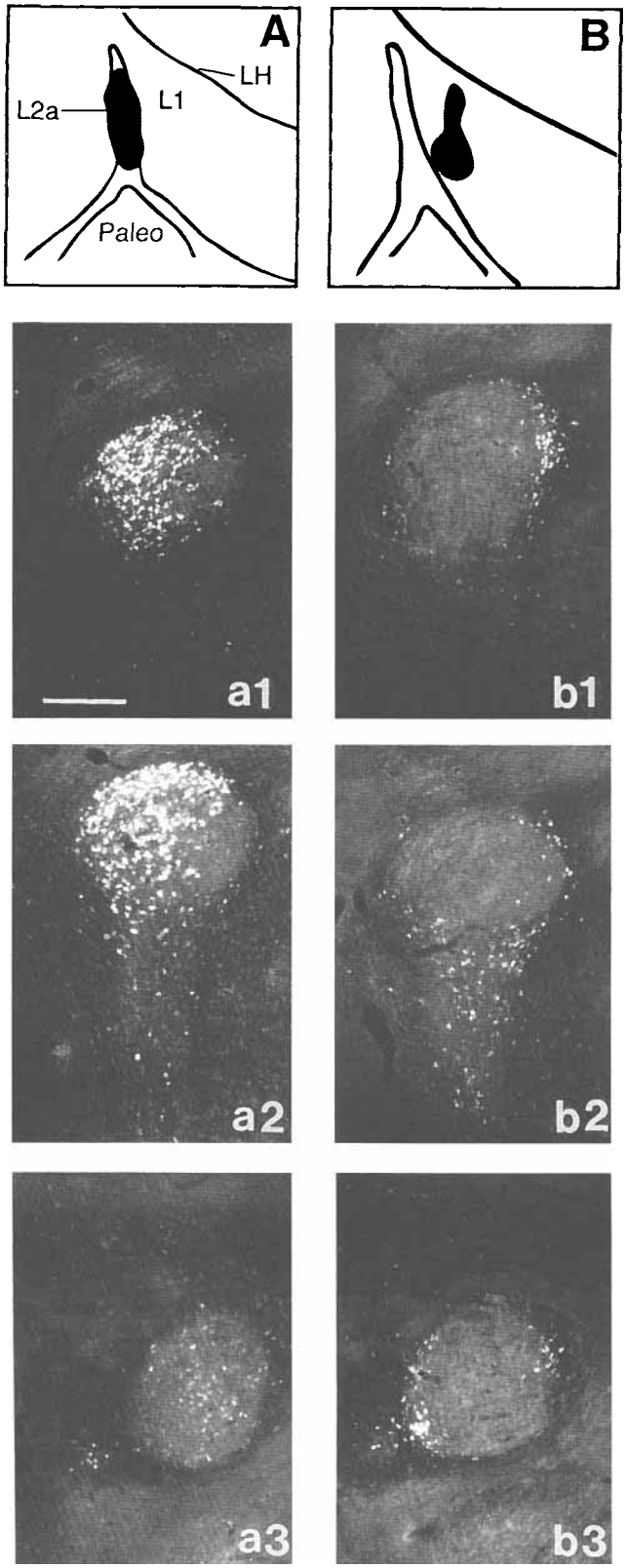

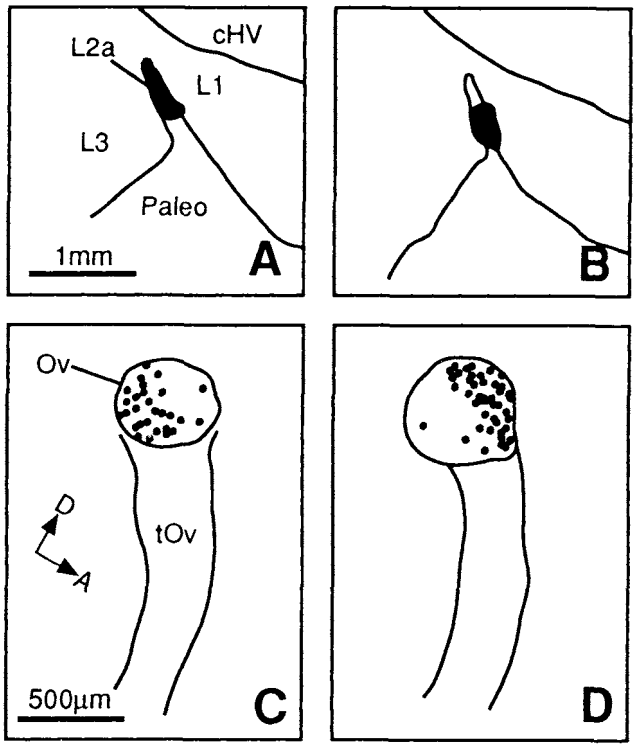

Fig. 6. Camera lucida drawings of parasagittal sections through the field L complex showing injection sites of beads into dorsal L2a (**A**) or BDA into ventral L2a (**B**) followed by drawings of corresponding parasagittal sections through the Ov complex (**C,D**) showing the different distribution of backfilled cells in Ov. For abbreviations, see list.

incoming fibers from L2a followed a straight path at right angles to the long axis of L2a, suggesting topographic connections between L2a and L1.

Injections of biocytin into ventromedial L2a showed a strong projection caudally to the rostroventral part of Ncm (Fig. 9). The distribution of labeled terminals from ventromedial L2a was very similar to the distribution of labeled fibers in Ncm after injection of anterograde tracer into Ov (cf. Fig. 3G). These fibers stopped at an easily identified border that left a caudal region of Ncm free of innervation from ventromedial L2a. In particular, injections into ventromedial L2a strongly labeled a band of fibers that was restricted to rostroventral Ncm (Fig. 9); in contrast, injections into dorsomedial L2a labeled fibers in rostrodorsal Ncm (not shown). This suggests a dorsoventral topography in the projection from medial L2a to rostral Ncm. Injections of beads and BDA limited to Ncm have confirmed that Ncm receives input from medial L2a (see below). However, these injections were not targeted specifically to either rostral or caudal Ncm; therefore, they could not confirm whether

Fig. 5. Camera lucida drawings of parasagittal sections through the field L complex showing injection sites of rhodamine-linked latex microspheres (beads) into L2a (**A**) or L1 (**B**) followed by corresponding lateral-to-medial series of photomicrographs through the Ov complex (**a1–a3** and **b1–b3**), demonstrating the different distribution of cells that project to L2a or L1, respectively. Injections of beads into L3 and the caudomedial neostriatum (Ncm) demonstrated a distribution of cells similar to that seen with injections into L1 (not shown). For abbreviations, see list. Scale bar = 500 µm.

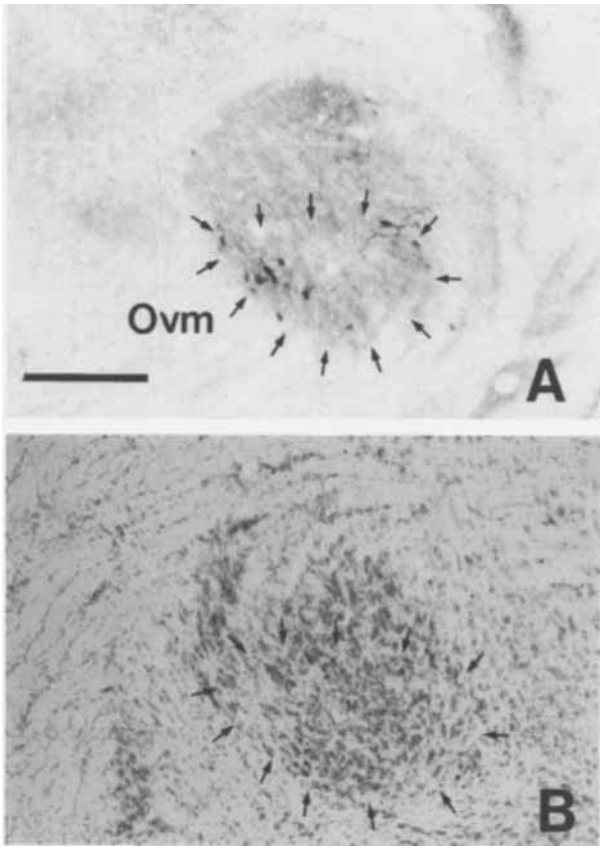

Fig. 7. Photomicrograph of a parasagittal section through the medial Ov complex (**A**) showing a small number of cells backfilled by injection of BDA into L2b (see Fig. 10). Examination of this and other sections confirmed that all backfilled cells were limited to the region delineated by arrows, the medial part of the nucleus ovoidalis (Ovm). The Nissl-stained alternate section (**B**) reveals a corresponding collection of neurons with larger cells bodies than the rest of Ov at this plane of section. Orientation is the same as in Figure 4. The medial part of Ov can be identified by its relation to the tractus occipitomesencephalicus (tOM), which defines the ventral and anterior border of Ov at this plane of section (compare to Fig. 3F). For abbreviations, see list. Scale bar = 150 μm.

medial L2a only projects to a specific region of Ncm, although they did corroborate the conclusion that the projection from medial L2a to rostral Ncm shows dorsoventral topography (not shown).

Injections of anterograde tracer that were limited to field L2a also showed a projection to PA and PP immediately ventral to L2a (Fig. 8F). For the most part, these fibers were straight and coursed ventrally from L2a through PA and PP; consequently, they might simply have been axons from cells in Ov that picked up tracer from injections into L2a. However, a small number of these fibers did follow a more convoluted path through PA and PP, with swellings indicative of presynaptic specializations. Thus, L2a may have a real projection to PA and PP, but we have not confirmed its existence by using retrograde tracers injected into PA or PP. In contrast to results in pigeon (Wild et al., 1993), no projection was observed from field L2a to visual Wulst or dorsal neostriatum. Also, injections of anterograde and retrograde tracers failed to demonstrate any direct connection between field L2a and the immediately adjacent song-control center NIf, a surprising finding considering the close anatomical proximity of NIf and L2a. There were occasional fibers that passed from L2a through NIf on their way to field L1, but these fibers did not seem to branch within NIf or to have any varicosities indicative of presynaptic specializations (not shown).

Injections of BDA as well as pure retrograde tracers into field L2a also showed numerous backfilled cells in fields L1 and L3 and in clHV (Fig. 8C–E). Because many of these cells were a relatively long distance from the injection site, we believe that they were not filled by local spread of the tracer to dendrites but, rather, that the connections of field L2a to many of its efferent targets are reciprocal. Injections of anterograde and retrograde tracers into these efferent targets of field L2a confirmed the reciprocal nature of the connections between field L2a and fields L1, L3, and clHV (see below).

Efferent projections of L2b

Figure 10 shows an injection of BDA into field L2b. Because the borders of field L2b were difficult to discriminate even in Nissl-stained sections, the decision that this and other injections were truly localized in L2b depended not only on comparisons to Nissl-stained alternate sections of tissue, but also on comparisons to similar tracer injections into fields L2a and L3 and into HVC shelf, which were the adjacent regions under investigation. For now, we describe the projections seen with these injections into L2b and, where appropriate, compare them to results from injections into these other adjacent regions of auditory neostriatum.

Injections of BDA and biocytin into L2b revealed that the most prominent output of L2b was directed to clHV (Fig. 10B). This projection was extremely dense and confined, showing labeled axon terminals in a well-limited area of clHV. This as well as other injections of BDA into L2b also revealed a number of backfilled cells in clHV in the same region that received the anterograde projection from L2b; other backfilled cells, however, were observed in parts of clHV that did not receive any input from L2b, suggesting that L2b only projects back to a subset of the cells in clHV that project to L2b. Of course, it is true that clHV sends projections that course through L2b on their way to other brain regions (see below) and that the cells backfilled in clHV after injection into L2b could have been backfilled as fibers of passage. However, as detailed below, anterograde injections into clHV showed a strong projection that terminated in L2b.

Injections of BDA and other anterograde tracers into field L2b also showed that L2b projects to both fields L1 and L3 (Fig. 10). This and other injections of BDA also revealed a number of backfilled cells in L1, L2a, and L3, confirming the projection from L2a to L2b seen with anterograde injections into L2a. However, as will be shown below, both L1 and L3 send projections to other brain areas that course through L2b but that do not appear to synapse in L2b. Therefore, the backfilled cells in L1 and L3 that were observed after injections into L2b may have picked up tracer via fibers of passage through the injection site.

Injections of anterograde tracers into field L2b also revealed a remarkable pattern of projections to paleostriatum (Fig. 10E,F). Fibers from field L2b terminated in PA, forming a ring around a vacant region of PP. The few fibers that did pass into PP were relatively straight and nonbranching, and they could have represented axons of backfilled cells in Ovm. We have not attempted to confirm retrogradely the projection from L2b to paleostriatum.

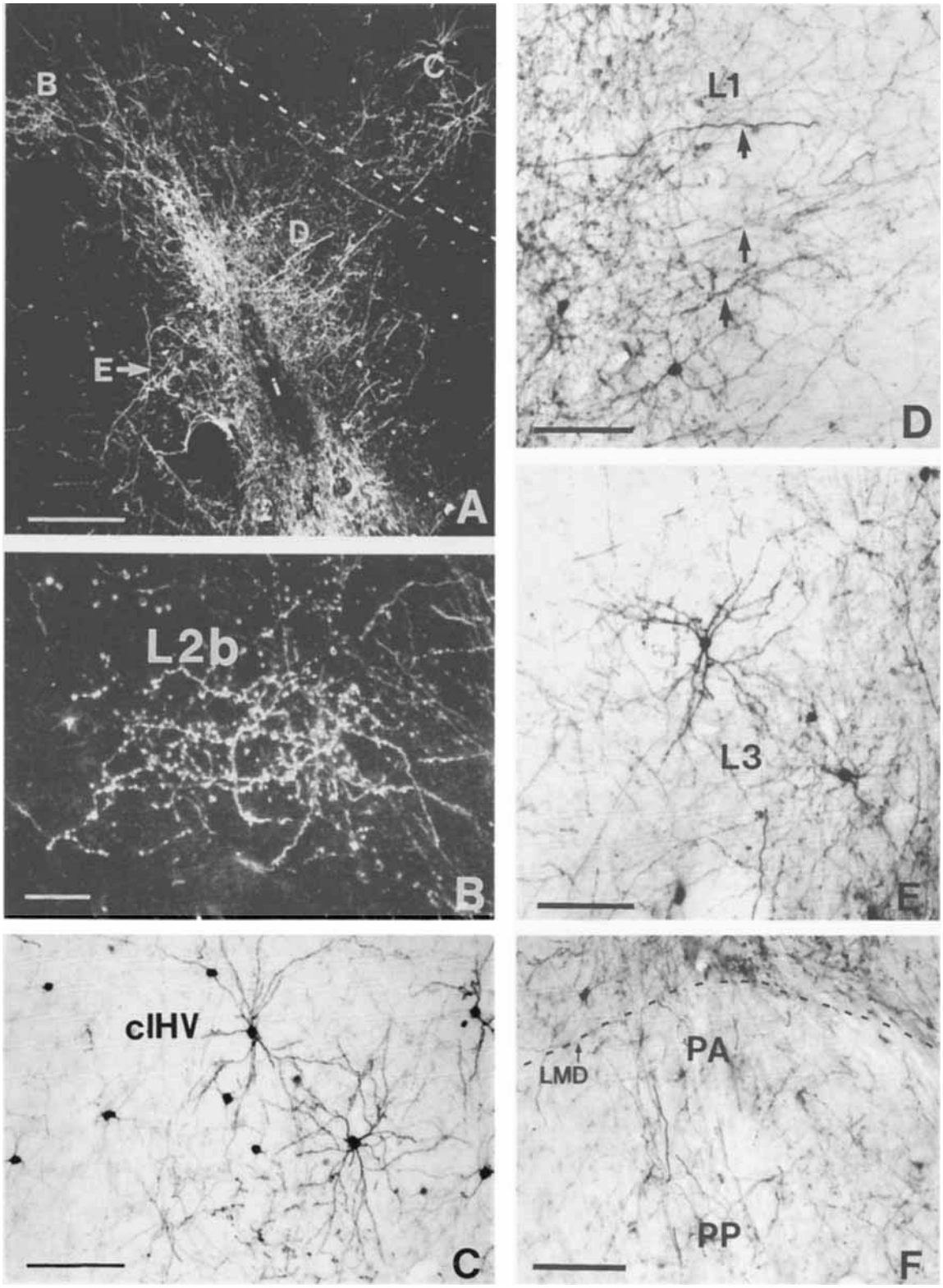

Fig. 8. **A:** Darkfield photomicrograph of an iontophoretic injection of BDA (i) into L2a. See Figure 1A for boundaries of the field L complex at this plane of section. Letters indicate the locations of the photomicrographs shown in B–F. The dashed line represents the lamina hyperstriatica (LH). **B:** BDA-labeled fibers and their varicosities in field L2b. **C:** Retrogradely labeled neurons in the caudolateral hyperstriatum ventrale (clHV). Note that there are also a number of very fine fibers in clHV. **D:** BDA-labeled fibers and their varicosities as well as retrogradely labeled neurons in L1. The arrows identify some labeled fibers that follow a very straight course within L1. **E:** BDA-labeled fibers and their varicosities as well as retrogradely labeled neurons in L3. **F:** BDA-labeled fibers in the paleostriatum augmentatum (PA) and the paleostriatum primitivum (PP). For abbreviations, see list. Scale bars = 300 μm in A, 50 μm in B, 100 μm in C–F.

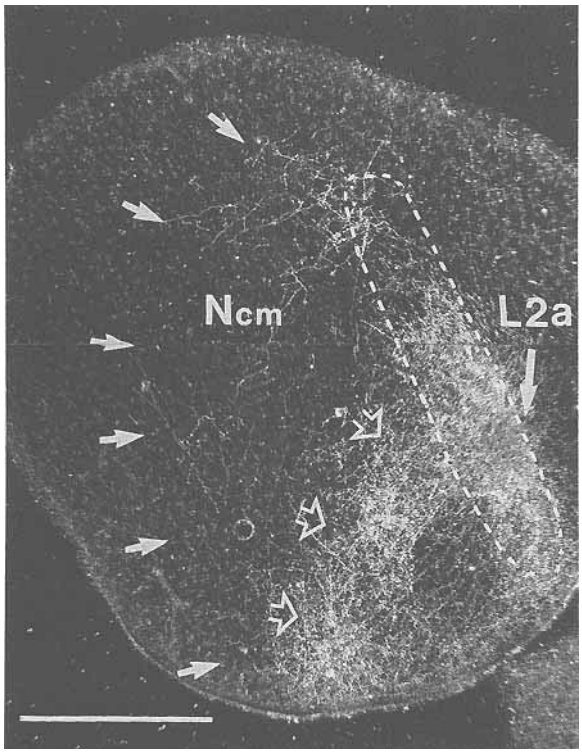

Fig. 9. Darkfield photomicrograph of an iontophoretic injection of biocytin into ventromedial L2a showing the pattern of anterograde labeling of fibers in Ncm. Open arrows show the boundary of the most intense labeling, which forms a curved band through rostral Ncm. The solid arrows indicate the boundary at which all labeling ends, leaving the caudalmost parts of Ncm free of labeling. Scale bar = 500 μm.

Interestingly, injections into field L2b showed almost no fibers projecting to the shelf of neostriatum immediately ventral to HVC (Fig. 10B). This supports our conclusion that injections targeted at L2b were indeed limited to L2b, and did not leak into neighboring HVC shelf, because any such leakage would have resulted in labeling of the rich interconnections within the HVC shelf (see below). Also, we conclude that our injections into L2b did not invade underlying field L3, because this would have resulted in labeling of the projection from L3 to the HVC shelf and the RA cup that is described later in this report, and no such labeling was ever seen with our injections into field L2b.

Telencephalic input to fields L1 and L3

Both fields L1 and L3, as described above, were observed to receive a strong projection from L2a. This was shown by injections of retrograde tracers into L1 and L3 that revealed backfilled cells in field L2a (Fig. 11). In addition, when field L1 was injected with retrograde tracers, backfilled cells were observed in field L3, and retrograde tracers injected into L3 revealed backfilled cells in L1 (Fig. 11). Thus, fields L1 and L3 are reciprocally interconnected. This was confirmed by using anterograde tracers (see below). The backfills of fields L1 and L3 generated by the injections of retrograde tracers described above revealed the same borders for fields L1 and L3 as those seen from injections of anterograde tracers in field L2a.

Injections of retrograde tracers in both fields L1 and L3 revealed a large number of labeled cells in clHV (Fig. 11). This differed significantly with Wild et al. (1993), who saw projections from cHV to field L2a in pigeon but found no evidence for a projection from cHV to fields L1 or L3. It could be argued that the backfilled cells seen in clHV after injection of retrograde tracers into L1 were cells whose axons traveled through L1 to L2a and whose fibers picked up tracers from L1 injection sites artifactually. However, this could not be true for cells in clHV that were backfilled by tracer injections into L3, because the injection sites in L3 were caudal to the terminations of fibers coming from clHV to L2a. In addition, injections of anterograde tracers into clHV confirmed the presence of a projection from clHV to fields L1 and L3 as well as to field L2a. Our results agree with Wild et al. (1993) in one respect: the cells in clHV that project to the field L complex were confined to the ventral part of clHV (Fig. 11).

Efferent projections of fields L1 and L3

Figure 12 shows an injection of BDA into field L1. From this injection and others, several efferent targets for L1 were identified. Two of these have already been discussed: the reciprocal connections between fields L1 and L2a and between fields L1 and L3. In addition, injections into field L1 revealed a rich projection to overlying clHV (Fig. 12C); this connection is reciprocal, because, as shown above, clHV projects to field L1 (Fig. 11). Although it is possible that fibers found in clHV after injections into field L1 may have represented leakage of tracer along the pipette track, injections of tracers into clHV confirmed that field L1 and clHV are reciprocally interconnected (see below). Injections into field L1 also showed some fibers in the neostriatum immediately anterior to L1 (not shown), but this projection has not been examined retrogradely. However, the strongest projection from L1 was directed to the neostriatum directly underneath HVC: the HVC shelf (Figs. 12A, 13). In Figure 13, the shelf under HVC can be defined by the anterogradely filled endings of fibers from field L1. Delineated in this way, the shelf is an irregularly shaped structure, and its thickness and configuration changes as one moves from medial to lateral and from posterior to anterior. These borders did not correspond to any obvious cytoarchitectonic borders in Nissl-stained material, although the fibers from field L1 stopped dorsally at the ventral boundary of HVC, as observed in Nissl-stained sections (not shown). The ventral border of the shelf, as defined by the projection from L1, did not dip deeper than 400–500 μm below the ventral border of HVC. However, its shape and distribution differed from the original definition of the shelf as the region immediately ventral and medial to HVC that received anterograde labeling from injections of tritiated amino acids into field L in canary (Kelley and Nottebohm, 1979) or as a thin parvocellular region tightly apposed to the ventral border of HVC (Nottebohm et al., 1982; Fortune and Margoliash, 1995). Injections of BDA and other retrograde tracers into HVC shelf have confirmed that many cells in field L1 project to the HVC shelf (Fig. 14).

Injections into L1 also showed a small number of fibers that penetrated HVC proper (Fig. 13B–D). The majority of these fibers appeared to arc through HVC on their way to the underlying shelf, but there were some that appeared to form swellings suggestive of presynaptic specializations. This would suggest that field L1 has a direct, albeit small, projection to HVC, which would be consistent with the report by Fortune and Margoliash (1995) of a direct projection from field L to HVC. Another possibility, however, is

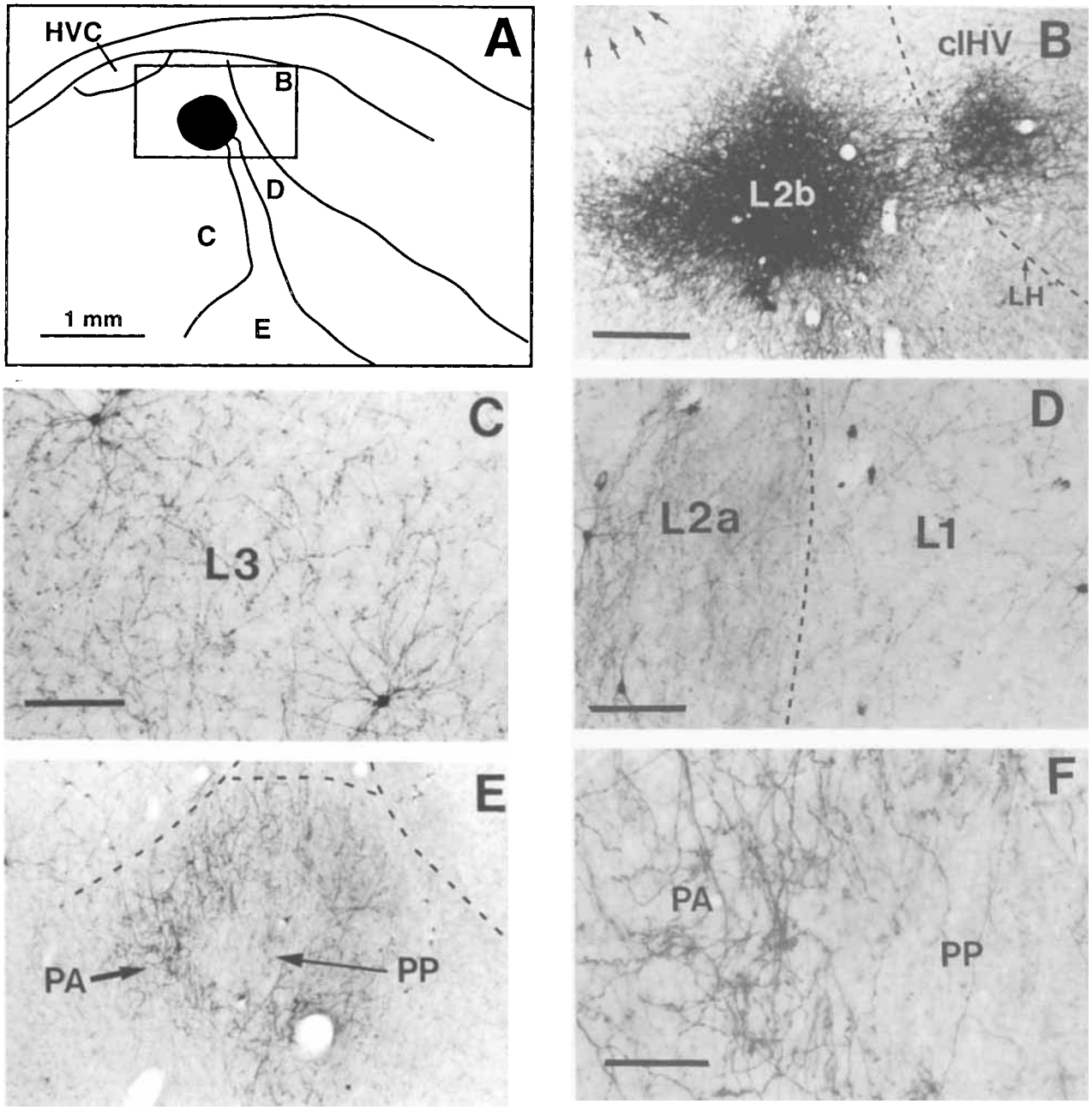

Fig. 10. **A:** Camera lucida drawing of an injection of BDA into field L2b. The rectangle shows the approximate field of view in B, whereas the rest of letters show the locations of C–F. See Figure 1A for boundaries of the field L complex at this plane of sections. **B:** Photomicrograph of injection site in field L2b showing intense anterograde labeling of fibers in clHV. Arrows mark a small part of the ventral border of the high vocal center (HVC). **C:** BDA-labeled fine fibers and retrogradely labeled neurons in L3. **D:** BDA-labeled fine fibers and retrogradely labeled neurons in L2a and L1. Note that fewer fibers are labeled than in L3. **E:** BDA-labeled fibers in paleostriatum resulting from the injection shown in B. **F:** Higher magnification photomicrograph of paleostriatum showing the different density of BDA-labeled fibers in PA and PP. For abbreviations, see list. Scale bars = 250 μm in B, 100 μm in C,D, 200 μm in E, 50 μm in F.

that fibers from NIf or from the medial part of the magnocellular nucleus of anterior neostriatum (mMAN), both of which project directly to HVC, may have taken up tracer from the L1 injection site. Attempts to confirm that HVC receives a projection from field L1 by using injections of retrograde tracers limited to HVC have revealed that a very small number of cells within field L1 can be backfilled from HVC (not shown). However, because injections into field L1 revealed fibers that pass through HVC without synapsing on their way to the shelf, it may be that some of these field L1 cells picked up tracers through their fibers of passage. We concluded that any projection from L1 to HVC is very small at best and, possibly, is not significant at all (see Discussion).

Large injections of anterograde tracers into field L1 also revealed a projection to Ncm that involved a small number

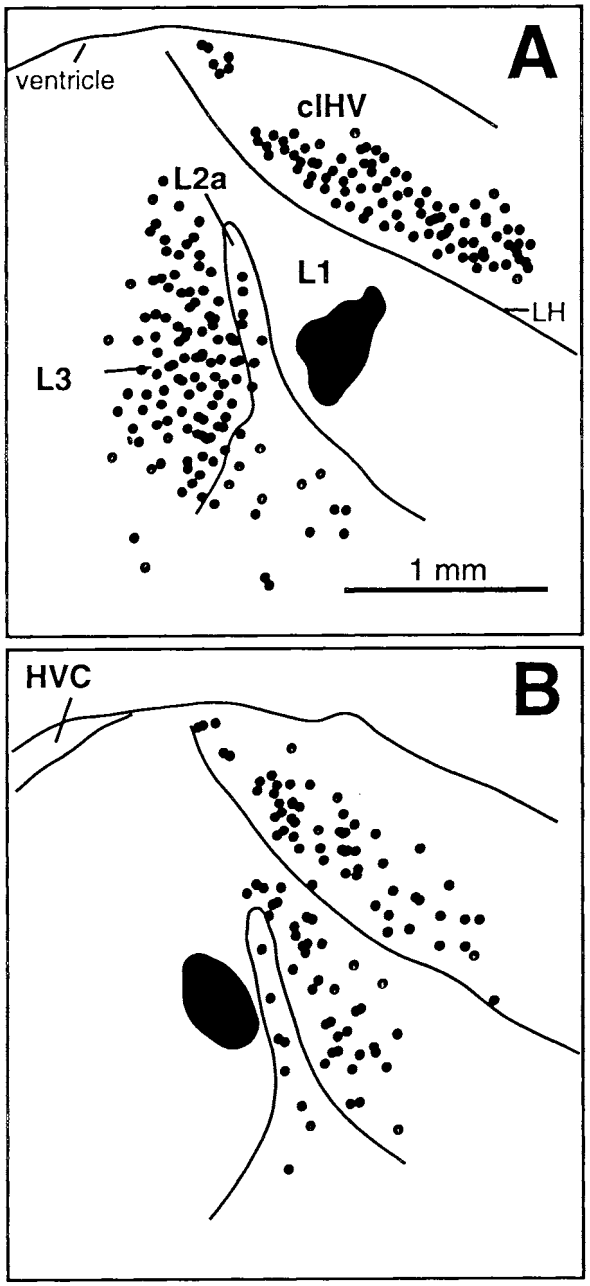

Fig. 11. **A:** Camera lucida drawing of an injection of beads into field L1 showing the distribution of retrogradely labeled cells in other parts of the field L complex as well as overlying clHV. Note that backfilled cells within L1 itself were observed but are not included in this figure. **B:** Camera lucida drawing of an injection of beads into field L3 showing the distribution of retrogradely labeled cells in other parts of the field L complex as well as clHV. Note that backfilled cells within L3 and overlying L2b were observed but are not included in this figure. For abbreviations, see list.

of fibers, even in large injections of L1 (not shown). However, we never injected tracers in the most medial extent of field L1 in order to avoid any chance of direct tracer spread into Ncm. Injections of retrograde tracers into Ncm failed to reveal backfilled cells in field L1. Consequently, it may be that the fibers in Ncm that were filled by injection of tracers into field L1 actually represented retrograde transport to branching axon collaterals of cells in field L3 that projected to Ncm (see below).

In addition, injections of anterograde tracers into field L1 revealed fibers in caudal paleostriatum (Fig. 12E). Interestingly, the labeled fibers from L1 were limited mostly to PA and did not ramify nearly as densely within PP; this distribution of labeled fibers was very similar to the pattern of projections from L2b (Fig. 10E). This projection was not confirmed by using retrograde tracers.

Injections into field L1 revealed a projection to the archistriatal region just anterior to RA: the RA cup (Fig. 12F). The fibers that formed this projection followed a trajectory that took them through the HVC shelf, from which they then descended towards the cup along the same arc traveled by the fibers descending from HVC to RA. Injections of BDA and beads into the RA cup have confirmed this connection by revealing retrogradely labeled cells in L1 (not shown).

The projections from field L3 mimicked those of field L1, with some important exceptions. Field L3, as described above, is reciprocally interconnected with L1, L2a, L2b, and clHV (Figs. 8, 10–12, 15). Interestingly, the projection from field L3 to clHV filled an oval area similar in shape and location to the area receiving projections from L2b (compare Fig. 15C to Fig. 10B). Field L3 also projected to the HVC shelf, but the pattern of fiber termination observed after injections into L3 involved a broader area of caudal neostriatum (Nc) underneath HVC, with a ventral border that stretched slightly farther ventrally and did not hold to the same shape as the area to which field L1 projected (Fig. 15D). This pattern of labeling, as before, did not correspond to any obvious cytoarchitectonic border in Nissl-stained sections, although it also respected the ventral border of HVC. The same injections of retrograde tracers into the shelf that backfilled neurons in field L1 also backfilled neurons (albeit a small number) in field L3 (Fig. 14). We did not attempt to inject retrograde tracers into regions where the L1 and L3 projections to shelf did not overlap; therefore, we cannot state with absolute certainty that there are portions of Nc underneath HVC that receive a projection from one, but not both portions of the field L complex. Like field L1, field L3 projects to the RA cup (Fig. 15); however, fibers labeled after injections into field L3 followed a different course from the fibers originating in L1. Rather than arcing through the HVC shelf, the fibers projecting from L3 to cup coursed caudally and ventrally from L3 through Nc, across the lamina archistriatalis dorsalis (LAD) that separates archistriatum from Nc, and towards the cup rostral to RA.

Injections of BDA and biocytin revealed that field L3 projects much more robustly to Ncm than field L1. Injections filled fibers that left the medial edge of L3, coursed towards the ventral surface of the caudal telencephalon, and then ascended dorsally when they reached Ncm. Figure 15F shows that the fibers from field L3 ramified widely within Ncm. However, they did not appear to evenly fill its entire extent, as defined by gene expression studies (Mello et al., 1992). Rather, the fibers were more dense in the ventral parts of Ncm. This suggests that parts of Ncm may differ on the basis of their afferents, as also seen with projections from Ov and medial L2a to Ncm (Figs. 3G, 9). However, this distribution of fibers did not conform to the uneven pattern of innervation of Ncm created by the projections from Ov and medial L2a, although it is possible that our injections into L3 did not reveal the full projection

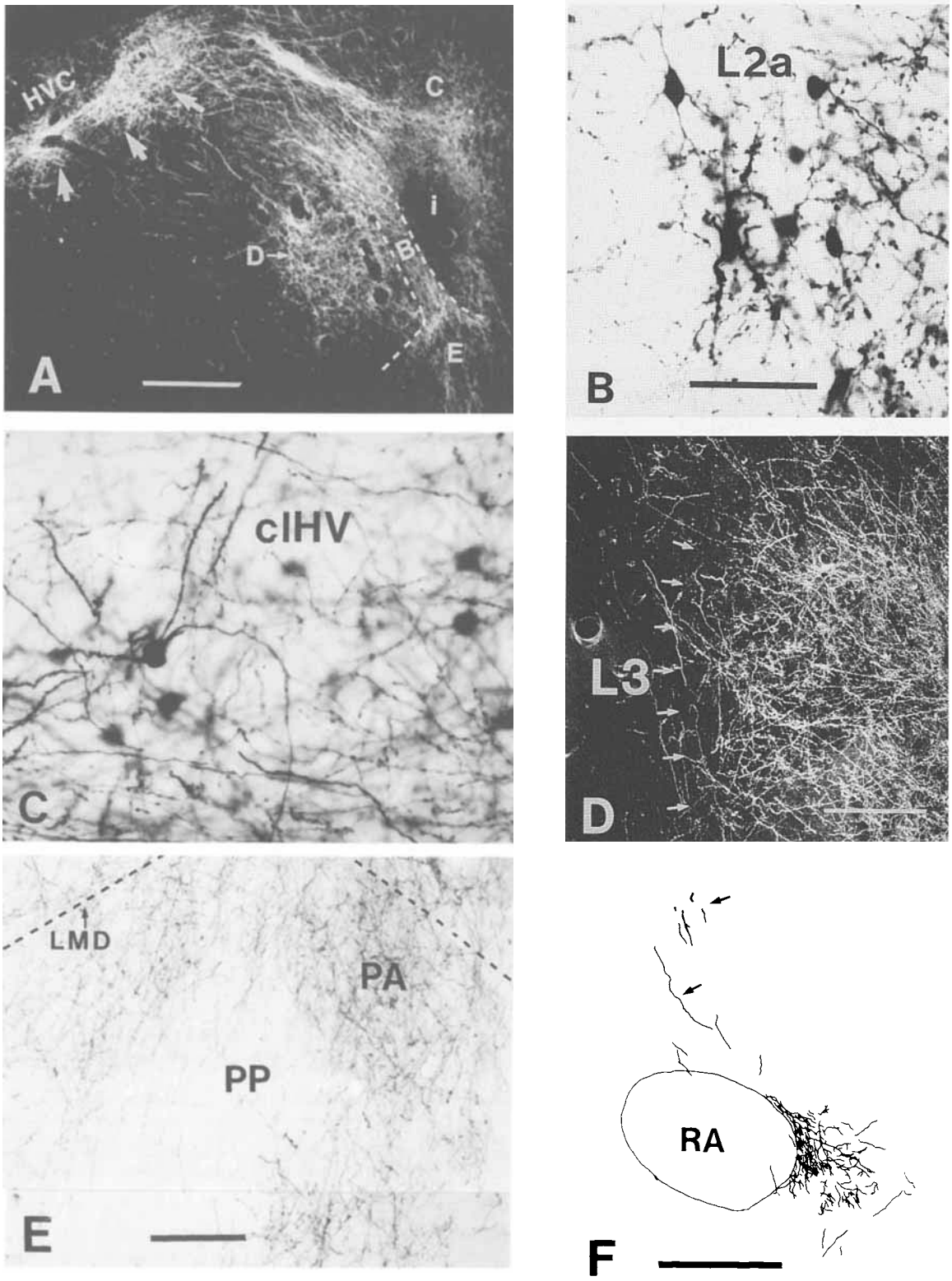

Fig. 12. **A:** Darkfield photomicrograph of an iontophoretic injection of BDA (i) into L1. Letters indicate the locations of the photomicrographs shown in B–E. Arrows indicate anterogradely labeled fibers in the HVC "shelf." **B:** Retrogradely labeled cells as well as labeled fibers in L2a. **C:** Retrogradely labeled cells as well as labeled fibers in clHV. **D:** Darkfield photomicrograph of BDA-labeled fibers in field L3. Arrows indicate the sharp caudal border of the densely labeled area, which corresponds with the border of L3 in Nissl-stained sections (not shown, but compare to Fig. 1A). There are also a number of retrogradely labeled cells in L3 that are not visible under darkfield illumination. **E:** BDA-labeled fibers in paleostriatum. **F:** Camera lucida drawing of BDA-labeled fibers in the archistriatum rostral to RA ("cup"). Arrows indicate fibers that descend from neostriatum below HVC towards the RA cup. Scale bars = 400 μm in A,F, 50 μm in B,C, 150 μm in D,E.

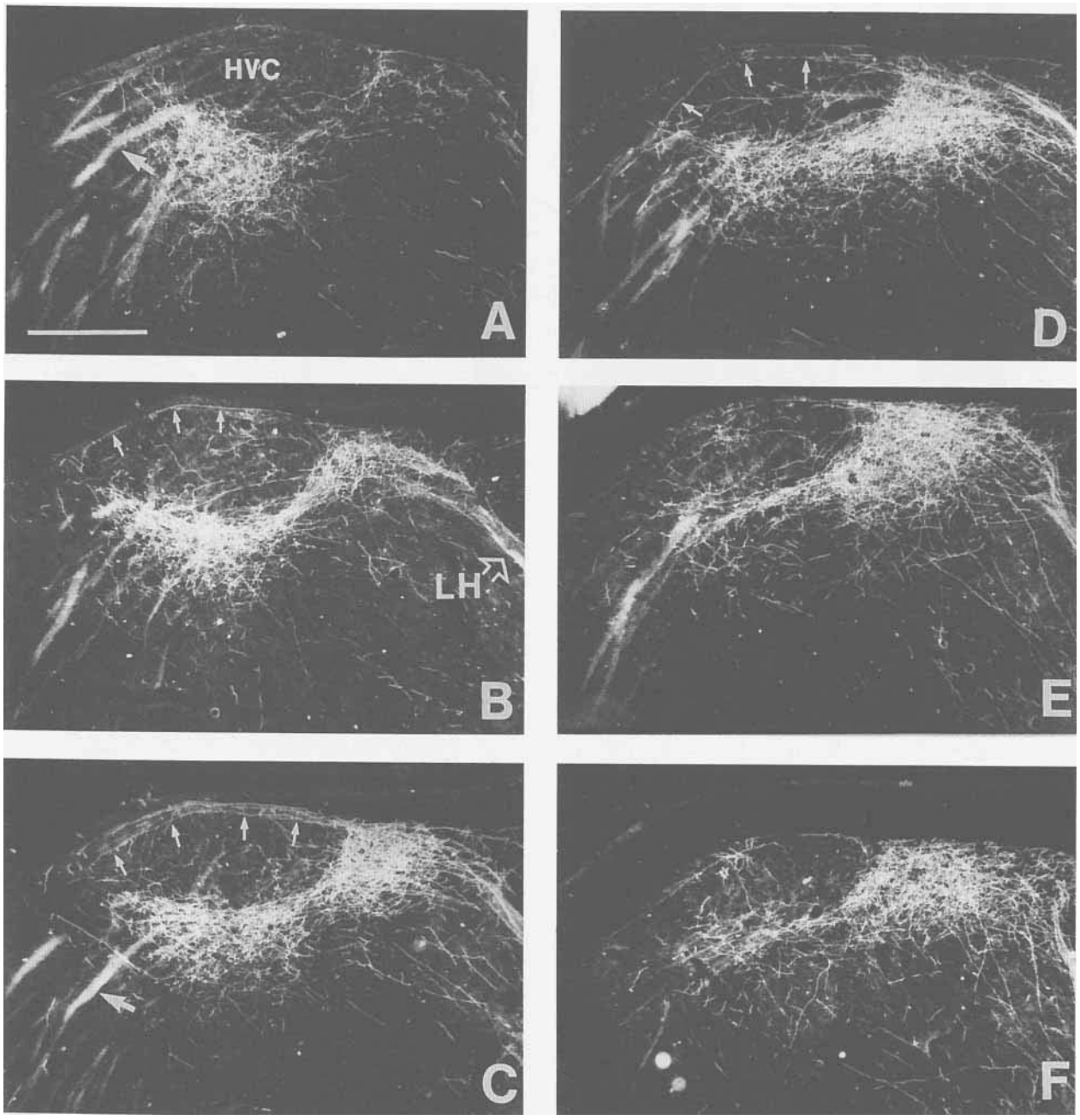

Fig. 13. **A–F:** A lateral-to-medial series of parasagittal darkfield photomicrographs (A is most lateral, and F is most medial; dorsal is up, and rostral is to the right) showing BDA-labeled fibers following an injection of BDA into L1 (see Fig. 12A). The vast majority of labeled fibers is within a specific region of neostriatum apposed to the ventral border of HVC—the HVC shelf. Projections from L1 to HVC shelf should not be confused with heavily myelinated fiber bundles leaving HVC for RA (large arrow in A,C). Note the relative absence of labeled fibers in HVC itself and that most of the labeled fibers in HVC seem to pass through in an arc (small arrows, B–D). Scale bar = 250 μm.

from L3 to Ncm. Large injections of retrograde tracers into Ncm confirmed that Ncm receives a strong input from field L3 (not shown), but no attempt was made to use smaller injections in order to confirm precisely whether different subregions of Ncm receive input from L3.

Inputs to Ncm

In addition to the input from auditory thalamus, medial field L2a, and field L3 described above (Figs. 3, 9, 15), injections of retrograde tracers into Ncm revealed that cmHV sends a strong projection to Ncm (Fig. 16). Injections of BDA in cmHV labeled axons that ramified widely throughout Ncm. Like most of the circuitry involving cHV, the connections between Ncm and cmHV are reciprocal, so that these same injections of BDA into cmHV also backfilled many cells within Ncm (see below). Backfilled cells were also observed in cmHV after injections of beads into Ncm (not shown). It should be noted that portions of clHV also projected to Ncm, but the number of fibers seen after injecting anterograde tracers into clHV was far smaller

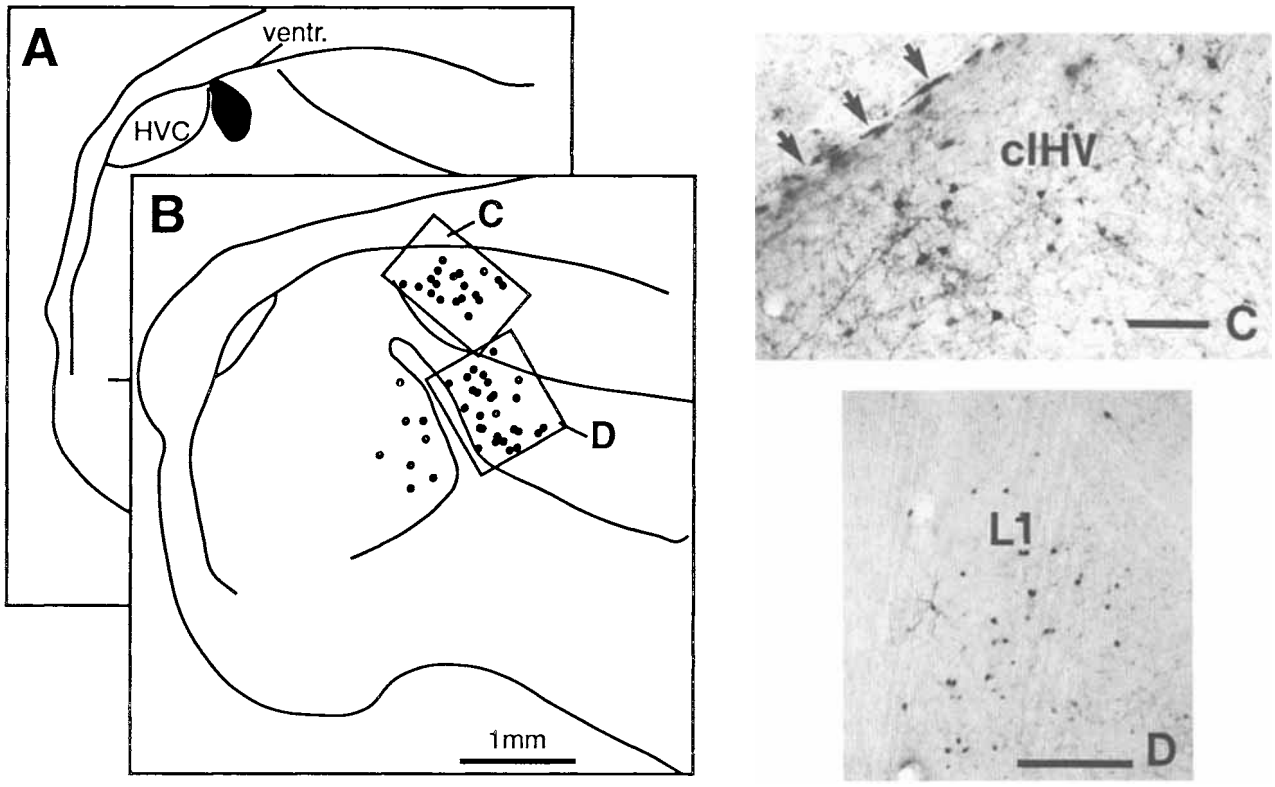

Fig. 14. **A:** Camera lucida drawing of an injection of BDA into the anterior HVC shelf. **B**: Camera lucida drawing of a section in the same brain ~400 μm more medial showing the location of the greatest density of retrogradely labeled cells in clHV, field L1, and field L3 (for orientation, refer to Fig. 1A). Note the absence of backfilled cells in L2b (i.e., dorsal and caudal of L2a). **C:** Photomicrograph of retrogradely labeled cells in clHV from the injection of BDA shown in A. The light labeling in the neuropil is background reactivity and does not represent labeled fibers. Arrows indicate the lateral ventricle overlying clHV. **D:** Photomicrograph of retrogradely labeled cells in field L1 from the injection of BDA shown in A. Ventr., lateral ventricle. Scale bars = 150 μm in C, 300 μm in D.

than after injecting into cmHV (see below). Also, the number of retrogradely labeled cells in clHV after injecting tracer into Ncm was much smaller than the number of retrogradely labeled cells in cmHV (Fig. 16F). Finally, the small injections of BDA in Ncm that revealed backfilled cells in cmHV also confirmed the dorsoventrally organized topographic projections of medial L2a to Ncm discussed above; for instance, the injection of BDA into dorsorostral Ncm shown in Figure 16A only labeled cells in the dorsal parts of medial L2a shown in Figure 16C. In contrast, injections into ventrorostral Ncm only backfilled cells in ventromedial L2a (not shown).

Injections of retrograde tracers into Ncm, as discussed above, revealed cells in the Ov shell and in tOv in a distribution similar to that seen with injections of retrograde tracers into L1 and L3 (not shown). In contrast, injections of retrograde tracers in the medial portion of L2a backfilled cells in the medial Ov core (not shown). However, the injections of retrograde tracers into Ncm were large and did not discriminate between the rostral parts of Ncm, which were seen to receive a projection from Ov with the use of anterograde tracers, and the caudal parts of Ncm, which did not receive such a projection. Therefore, it is possible that the backfilled cells that were observed in Ov shell after injections into Ncm projected only to the rostral part of Ncm.

Efferent projections of Ncm

Figure 16 shows an injection of BDA into Ncm. This and other injections of anterograde tracers showed that Ncm is richly interconnected within itself (Fig. 16B) and sends a strong projection to cmHV (Fig. 16D). Injections of retrograde tracers limited to cmHV confirmed the presence of a projection from Ncm (see below). It is interesting to note that the reciprocal connection between Ncm and cmHV is strongly limited in the mediolateral plane, i.e., Ncm projects only to parts of cHV within 750 μm of the midline (cmHV) and not to the more lateral clHV. This was best appreciated in frontal sections, where injections of BDA into Ncm revealed that the projection to cmHV only penetrated approximately 700 μm laterally (Fig. 16E,F). Also, the majority of backfilled cells were present in cmHV and not in clHV. Thus, the labeled fibers from Ncm served to identify cmHV as an anatomically specialized subregion of cHV.

In addition to the projection from Ncm to cmHV, anterograde injections into Ncm filled a smaller number of fibers that penetrated far laterally into parts of Nc that did not overlap with L3 or the HVC shelf (not shown). The connectivity of these lateral Nc regions has not been explored further.

Afferents of cHV

Caudal HV, as far lateral as the center of HVC (approximately 1.9 mm from the midline), receives input from underlying auditory neostriatum. Injections of different tracers have revealed that clHV receives input from and projects back to the underlying field L complex (Figs. 8, 10–12, 15, 17). In contrast, cmHV receives its input from Ncm rather than from the field L complex, as shown by

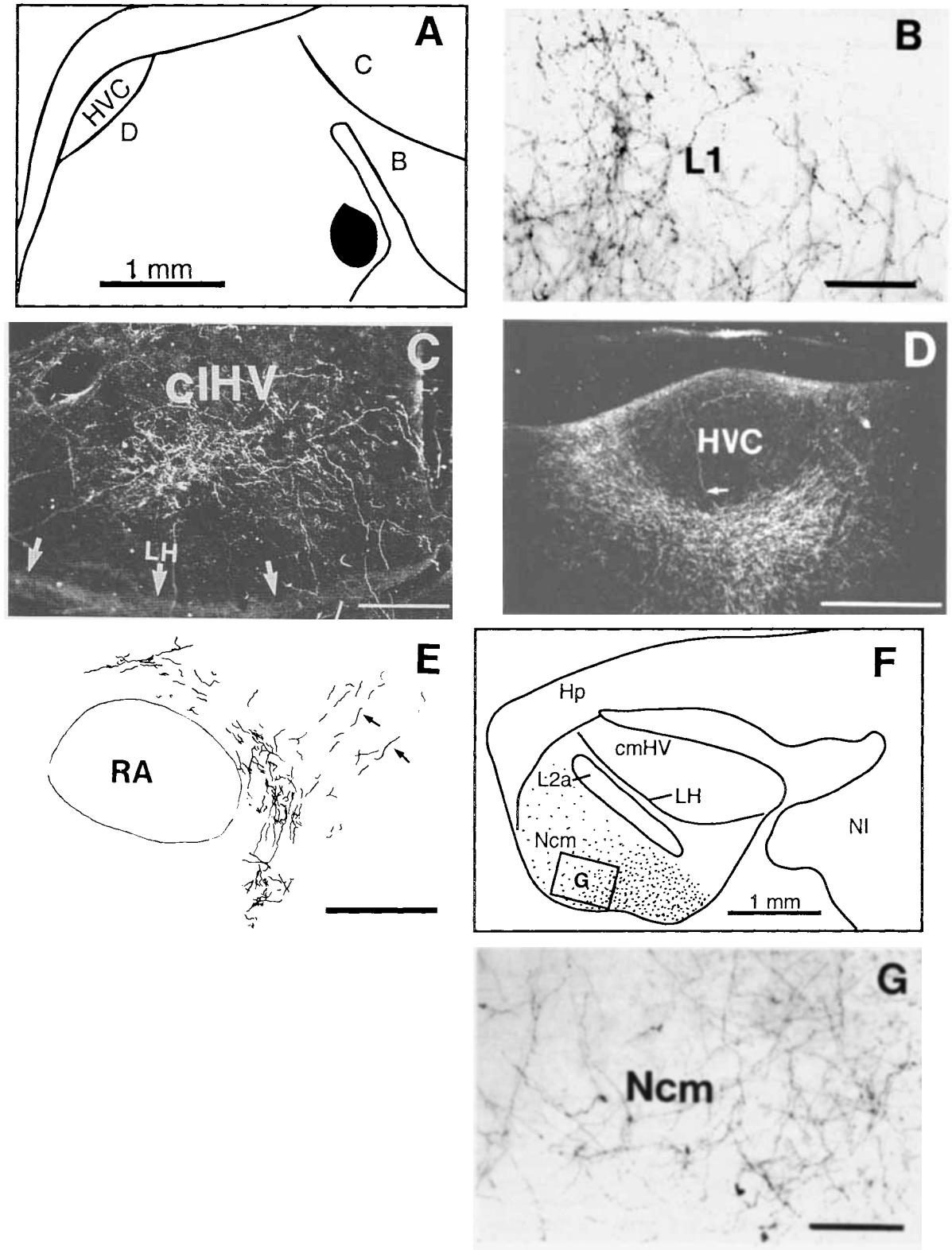

Fig. 15. **A:** Camera lucida drawing of an injection of biocytin into field L3. Letters indicate the positions of the micrographs shown in B–D. **B:** Biocytin-labeled fibers with varicosities in field L1. There are no retrogradely labeled cells, because biocytin is a purely anterograde tracer. **C:** Darkfield photomicrograph of biocytin-labeled fibers in clHV. Arrows indicate the location of LH, which forms the ventral border of clHV. **D:** Darkfield photomicrograph of biocytin-labeled fibers in HVC shelf. This particular section is approximately 300 μm lateral of the injection site. Arrow indicates one fiber that enters the body of HVC. **E:** Camera lucida drawing of BDA-labeled fibers in the archistriatum rostral to RA (cup). Arrows indicate fibers that course towards the RA cup directly from the injection site in L3, rather than arcing dorsally below or through HVC before descending towards the archistriatum like the fibers from L1. **F:** Camera lucida drawing of a brain section ~400 μm from the midline showing the distribution of biocytin-labeled fibers in Ncm. The density of stippling corresponds roughly to the density of labeled terminals. **G:** Biocytin-labeled fibers with varicosities in the part of Ncm delineated by the rectangle in F. For abbreviations, see list. Scale bars = 100 μm in B,G, 200 μm in C, 400 in D,E.

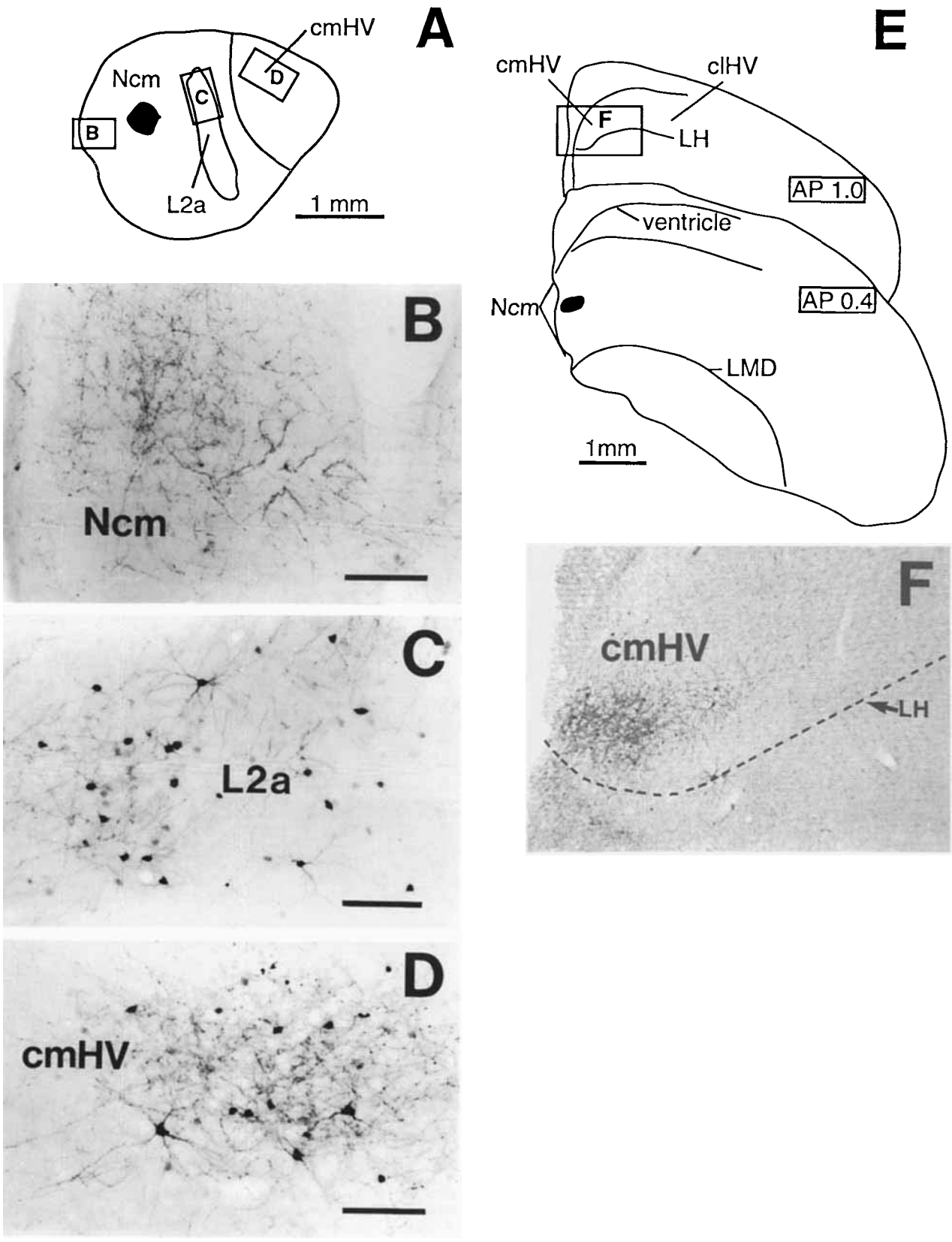

Fig. 16. **A:** Camera lucida drawing of a parasagittal section through caudal telencephalon ~ 300 μm from the midline, showing an injection of BDA into Ncm. Rectangles correspond to the photomicrographs shown in B–D. **B:** BDA-labeled fibers in caudal Ncm. Although this particular photomicrograph does not show any retrogradely labeled cells, the injection did backfill some cells in caudal Ncm. **C:** Retrogradely labeled cells and anterogradely labeled fibers in medial L2a. **D:** Retrogradely labeled cells and anterogradely labeled fibers in cmHV. Labeling is limited to a discrete field within cmHV. **E:** Camera lucida drawing of two frontal sections through the caudal telencephalon showing an injection of BDA into Ncm (AP 0.4) and the area of caudal HV (cHV) rostral to the injections site (AP 1.0), which is shown in F. **F:** BDA-labeled cell processes and retrogradely labeled cells in cmHV resulting from the injection shown in E. For abbreviations, see list. Scale bars = 100 μm in B–D, 250 μm in F.

injections into cmHV that revealed backfilled cells only in Ncm, and by injections of anterograde tracers in Ncm (Figs. 16, 18). Small injections of anterograde and retrograde tracers in clHV and cmHV also indicated that cHV is richly interconnected within itself over the mediolateral extent from Ncm to field L; this was best appreciated in frontal sections (Fig. 18C–F). Injections of retrograde tracers into cmHV and clHV revealed a very small number of backfilled cells in the Ov shell (not shown); this was in accord with reports by others (Durand et al., 1992; Wild et al., 1993) of a direct connection between the Ov surround and HV in nonsongbird species. Our injections of anterograde tracers into the Ov complex showed a few labeled fibers in cHV (not shown). Also, our injections into clHV did not reveal any backfilled cells in or near Uva. In contrast, Fortune and Margoliash (1995) observed backfilled cells surrounding Uva after injections of tracers into what they termed HV. However, the area they targeted in their injections was rostral to the area we have identified as clHV (see Fortune and Margoliash, 1995; Fig. 22); therefore, these two sets of data need not be contradictory. However, Fortune and Margoliash (1995) did not use anterograde tracers to confirm the projection from the area surrounding Uva to HV. In the absence of anterograde confirmation, we believe that the connection from areas surrounding Uva to what they call HV awaits confirmation.

Efferent connections of cHV

The reciprocal connections between clHV and the field L complex and between cmHV and Ncm have been documented above, but the mediolateral specificity of their projections is best appreciated in frontal sections (Fig. 18C–F). Anterograde injections into clHV labeled fibers in all parts of the field L complex (Figs. 17A, 18F) but labeled only a few fibers to Ncm; in contrast, anterograde injections into cmHV showed a robust projection to Ncm (Fig. 18B,E) but very few labeled fibers in parts of the field L complex. Injections of anterograde tracer into clHV also showed a particularly robust projection to L2b (Fig. 17A). Because field L2b was difficult to define in Nissl-stained sections, it is possible that this projection may have involved a larger area than L2b alone; but, at the very least, it suggests that clHV projects more heavily to the parts of Nc that include field L2b than to fields L1, L2a, or L3. Anterograde injections into clHV also labeled fibers throughout much of cHV itself; frontal sections show that a BDA injection site in clHV at 1.6 mm from midline labeled axons that run to cmHV (Fig. 18D,F). A similar injection into cmHV labeled fibers that stretched laterally to the same level as the previously described injection site in clHV (Fig. 18C,E).

Anterograde injections into clHV also revealed a robust projection to the HVC shelf (Fig. 17C). Although this projection overlaps significantly with the projections from fields L1 and L3, it concentrates on the more anterior reaches of the shelf. The projection from clHV to anterior shelf has been confirmed by comparing backfills of clHV after injection of retrograde tracer into the rostral or caudal shelf. Injections into the caudal shelf failed to backfill more than a few of neurons in clHV (not shown), whereas injections into the anterior shelf backfilled many more neurons in clHV (Fig. 14).

Surprisingly, injections of anterograde tracers into clHV also revealed a small number of fibers penetrating into HVC itself (Fig. 17C) as well as a strong projection to NIf (Fig.

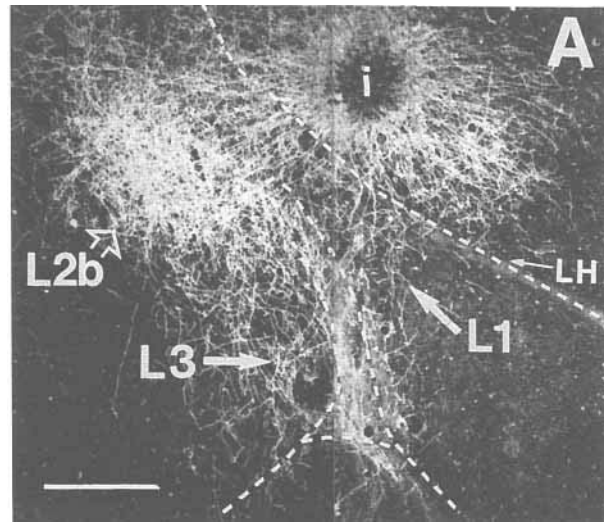

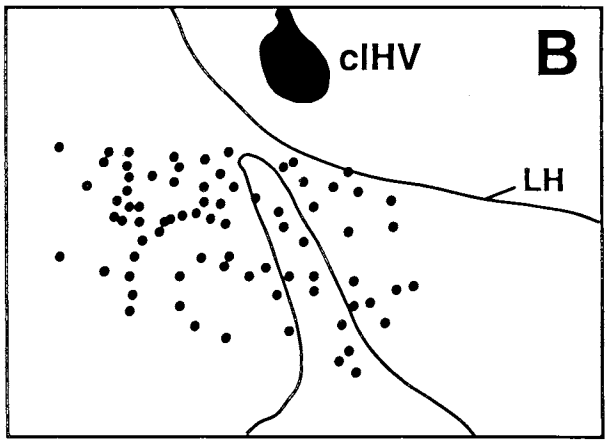

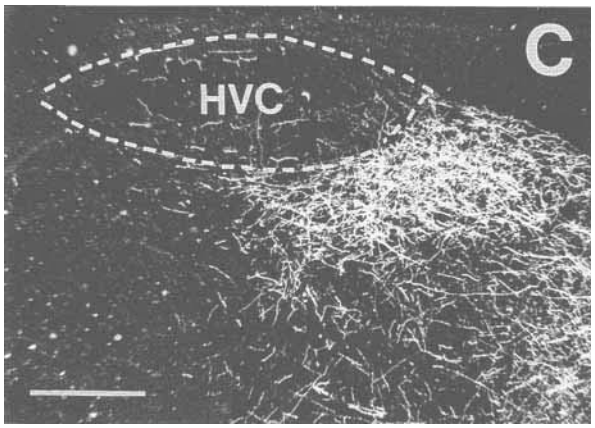

Fig. 17. **A:** Darkfield photomicrograph of a parasagittal section showing an iontophoretic injection of BDA (i) into clHV. Fields L1, L2a, and L3 all contain BDA-labeled fibers, but the greatest density of labeled fibers is in L2b, located dorsocaudal to the tip of L2a. **B:** Camera lucida drawing of a parasagittal section at the same mediolateral level and scale as A in a different brain injected with beads into clHV showing the distribution of backfilled cells in the field L complex. **C:** Darkfield photomicrograph of a parasagittal section ~300 μm lateral to A showing BDA-labeled fibers in the rostral HVC shelf. Dashed lines indicate the borders of HVC. Scale bars = 500 μm in A, 300 μm in C.

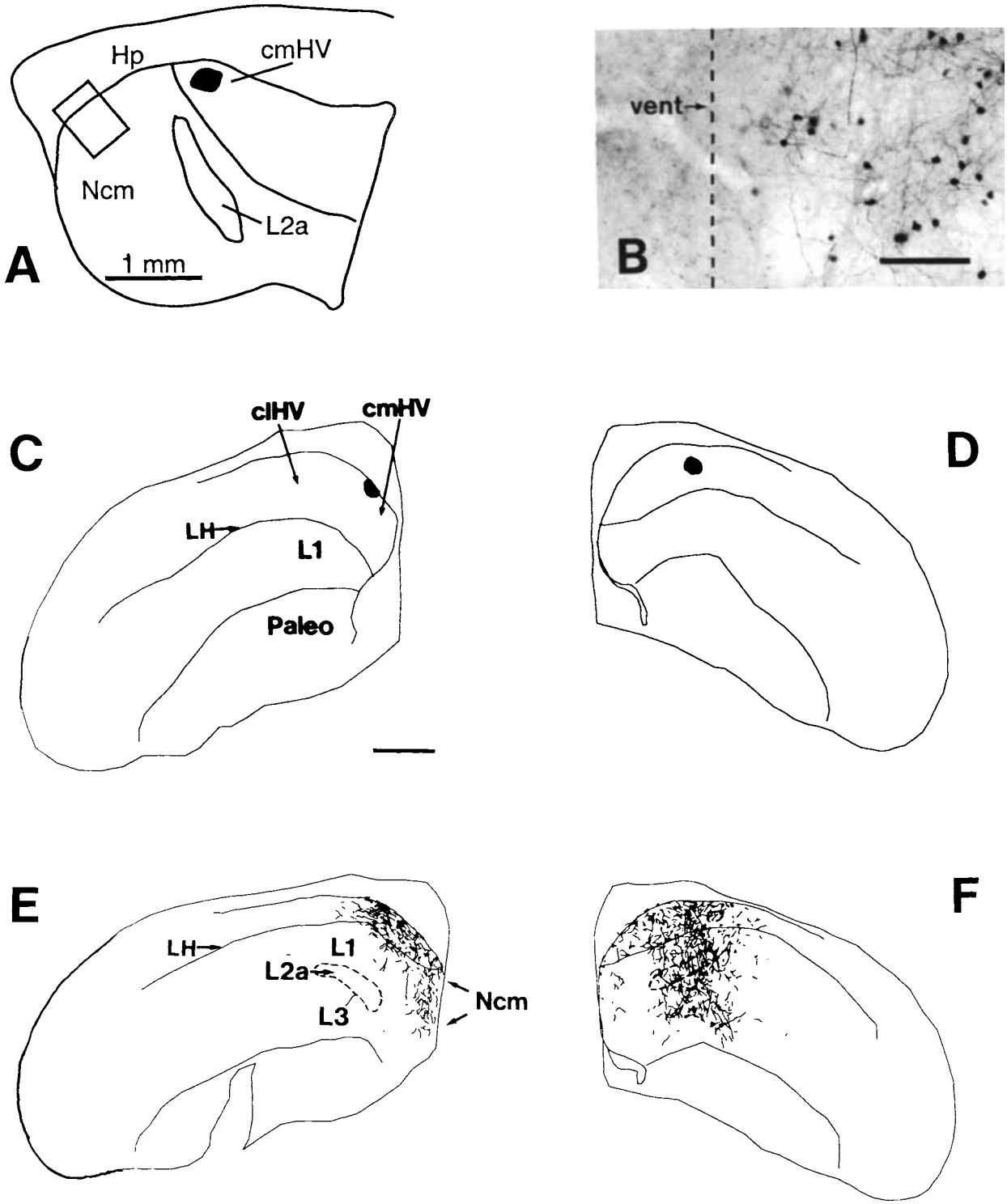

Fig. 18. **A:** Camera lucida drawing of a parasagittal section ~500 μm from the midline showing an injection of BDA into cmHV. Rectangle marks the approximate area of Ncm shown in B. **B:** BDA-labeled fibers and retrogradely filled cells in Ncm. **C:** Camera lucida drawing of a frontal section showing an injection of BDA into cmHV (~500 μm from the midline). **D:** Camera lucida drawing of a frontal section showing an injection of BDA into clHV (~1.6 mm from the midline). **E:** Camera lucida drawing of a frontal section ~300 μm caudal to C showing BDA-labeled fibers in Ncm and in the most medial parts of the field L complex. Labeled fibers can also be traced within clHV > 1.5 mm from the midline, but there are very few labeled fibers in neostriatum > 1 mm from the midline. **F:** Camera lucida drawing of a frontal section ~300 μm caudal to D showing BDA-labeled fibers in all parts of the field L complex. Labeled fibers can be traced well into cmHV, but there are very few labeled fibers within Ncm. Vent, lateral ventricle. For abbreviations, see list. Scale bars = 100 μm in B, 1 mm in C.

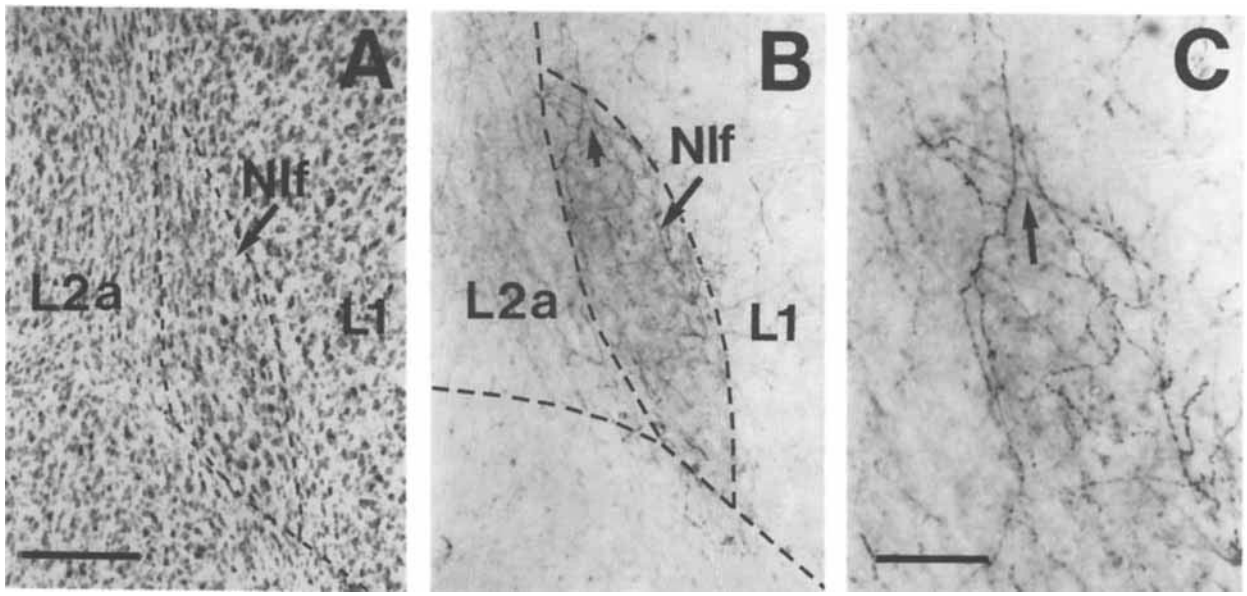

Fig. 19. **A:** Nissl-stained parasagittal section from the clHV-injected brain in Figure 17 showing the location of the song circuit center NIf in relation to parts of the field L complex. Refer to Figure 1A for orientation. **B:** The next section lateral showing BDA-labeled fibers in NIf resulting from the injection into clHV shown in Figure 17. **C:** Higher magnification of labeled processes in NIf showing how the fibers respect the borders of NIf and are thicker than the few fine fibers in adjacent L2a and L1. The arrow in C corresponds to the small arrow in B. Scale bars = 100 μm in A, 50 μm in C.

19), which is known to project directly to HVC (Nottebohm et al., 1982). Attempts to confirm that HVC receives a direct projection from clHV were confounded by the spread of most conventional retrograde tracers (e.g., beads and FLG) out of HVC into the shelf. We addressed this problem by making small iontophoretic injections of BDA and RDA that were limited strictly to HVC; however, these did not demonstrate any backfilled cells in clHV. Consequently, we concluded that our injections of anterograde tracers into clHV may have labeled fibers of passage from mMAN, a known afferent to HVC whose fibers largely pass through the underlying LH to enter HVC at its rostral pole; mMAN cells were backfilled by the same injections into HVC that failed to backfill any cells in clHV. In contrast, we are confident that clHV projects to NIf, because the only afferent of NIf described previously is Uva (Nottebohm et al., 1982; Williams, 1989), and the fibers from Uva reach NIf from below and do not come anywhere near clHV. In addition, the fibers from clHV that terminated in NIf had numerous varicosities that suggested presynaptic specializations. To confirm that clHV projects to NIf, we placed small iontophoretic injections of BDA targeted at NIf. Because of NIf's convoluted structure, it was impossible to fill NIf entirely without risking leakage into surrounding parts of field L. However, small injections into lateral NIf (Fig. 20A) that filled only less than one-third of the nucleus still revealed a small but significant number of backfilled cells in clHV (Fig. 20B, inset). In addition, these injections anterogradely labeled the known target of NIf's projection, which is HVC (Fig. 20C), and retrogradely labeled cells in Uva, which is the known afferent of NIf (Fig. 20D). We believe that the absence of anterograde fiber labeling in any of the known targets of fields L2a or L1, as well as the absence of retrograde labeling in Ov support our conclusion that these injections into NIf did not leak significantly into adjacent fields L2a or L1, and that the backfilled cells in clHV confirmed the projection to NIf.

Injections of anterograde tracers in clHV labeled a small number of fibers in the RA cup (not shown). However, this projection may be more robust than indicated by these small injections, because injections of retrograde tracers in the cup backfilled a large number of neurons in clHV (not shown). This connection will be addressed further in a later paper (Mello and Vates, unpublished observations).

Connections of the HVC shelf and its relationship to HVC

Fields L1 and L3, and clHV provide strong inputs to the HVC shelf, as described above (Figs. 13–15, 17). For the most part, these afferents to the shelf send projections that are restricted to an area of neostriatum extending no more than 500 μm ventrally from HVC. However, the specific terminal fields of projection from L1, L3, and clHV that were shown by our injections of anterograde tracers varied widely in their shape. These differences in the distribution of terminations from these three centers suggest that the shelf is not a unitary structure but, rather, a complex auditory center receiving different relative amounts of input from areas in the field L complex and the clHV in anatomically distinct subregions.

Injections of anterograde tracers into the HVC shelf were remarkable in that they showed a rich pattern of interconnections within the shelf itself and also demonstrated that the shelf is anatomically distinct from HVC. Injections of biocytin and BDA that were limited to the shelf labeled axons that coursed caudally and rostrally to innervate almost the whole shelf within one parasagittal plane of section (Fig. 21). The wide dispersal of axons within the shelf is consistent with data from intracellular injections of

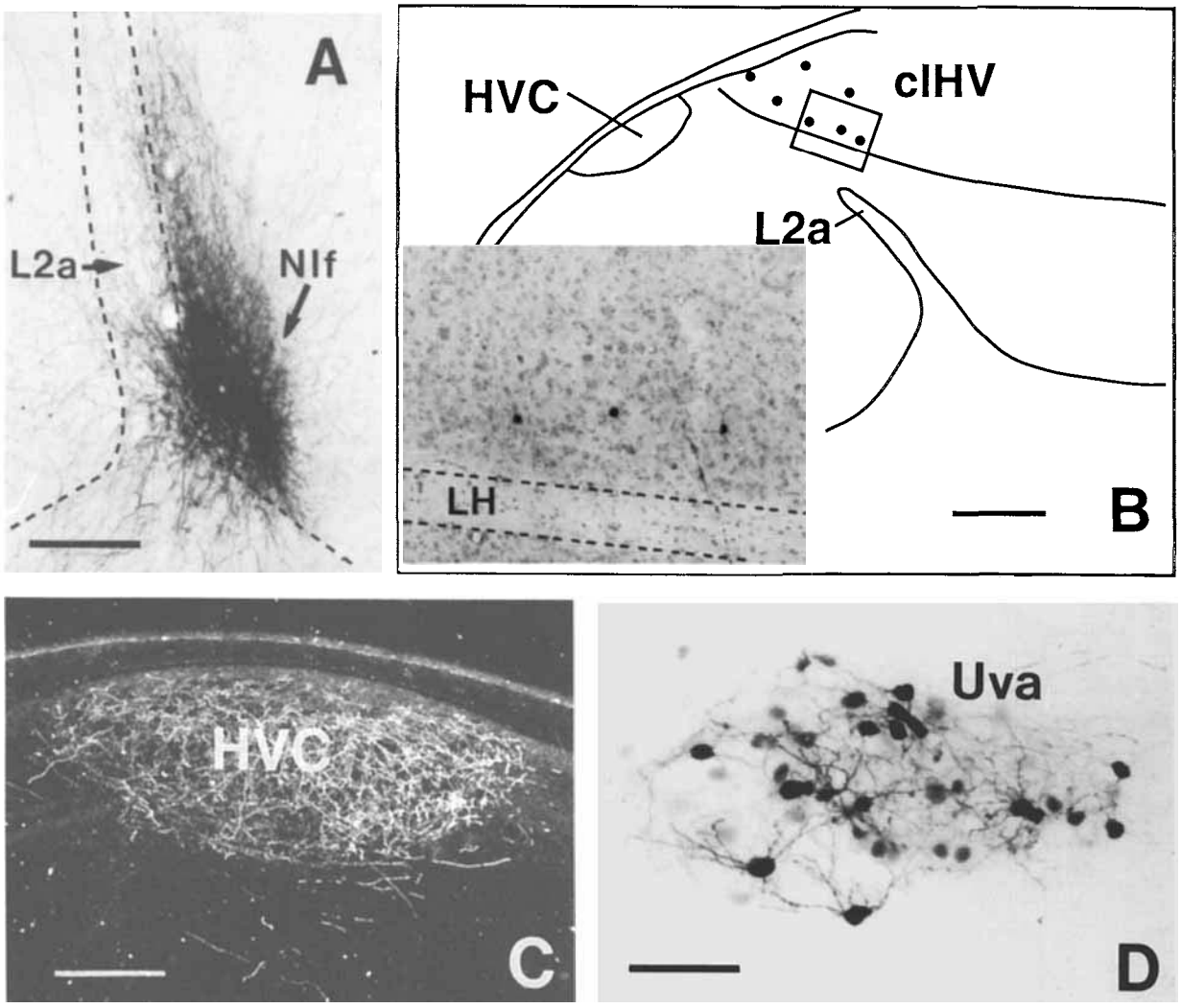

Fig. 20. **A:** Injection of BDA into NIf shown in parasagittal section. The injection fills only a portion of NIf; the labeling dorsal to NIf represents fibers ascending towards HVC. This small iontophoretic injection shows little if any leakage into L1 dorsorostrally, into L2a caudally, or into paleostriatum ventrally. **B:** Camera lucida drawing of a parasagittal section ~300 μm lateral to the injection site showing the location of the highest density of retrogradely labeled cells in clHV. At this location, NIf is no longer evident. The rectangle indicates the area of clHV shown in the **inset**, which reveals backfilled cells in clHV. **C:** BDA-labeled fibers in HVC resulting from the injection shown in A. **D:** Retrogradely labeled cells in the nucleus uvaeformis of the thalamus (Uva), which innervates NIf and HVC. For abbreviations, see list. Scale bars = 100 μm in A, 400 μm in B, 200 μm in C, 50 μm in D.

tracers into shelf neurons (summarized by Margoliash, 1987). Interestingly, axons could also be followed medially and laterally within the shelf, but the reach of axons in the mediolateral axis was not as prominent as in the rostral-caudal dimension of the shelf. This matches well with observations of the rostrocaudal coursing of myelinated fibers underneath HVC using Nomarski optics (Fortune and Margoliash, 1995). Thus, the shelf may be organized in a series of discrete domains along the mediolateral axis. Injections into neostriatum 800–1,200 μm under HVC did not label a significant number of fibers in shelf (not shown), supporting the idea that the neostriatum within 500 μm of the ventral HVC border is an anatomically discrete region. Anterograde injections into field L2b, which is just ventral to the rostral part of the shelf, showed no labeled fibers within the shelf and confirmed the ventral border of the shelf in that region (Fig. 10B).

Injections of anterograde tracers in the HVC shelf showed a small number of fibers penetrating into HVC (Fig. 22). We have observed that iontophoretic injections placed immediately under the ventral border of HVC revealed an incredibly discrete border between HVC and shelf that appeared to be virtually inviolable to the local spread of these tracers, similar to the way these same tracers respected the borders between field L2a and the flanking regions L1, L3, and NIf. Consequently, we feel confident that some of the few fibers seen in HVC represented axons from shelf cells coursing into HVC. For the most part, these axons ran within the parasagittal plane of section, again implying a possible mediolateral organization in the projections between the shelf and HVC. However, the number of axons was very limited, and indeed injections of BDA that largely filled HVC only rarely backfilled any cells in the shelf (not shown). However, some injections into HVC were notable,

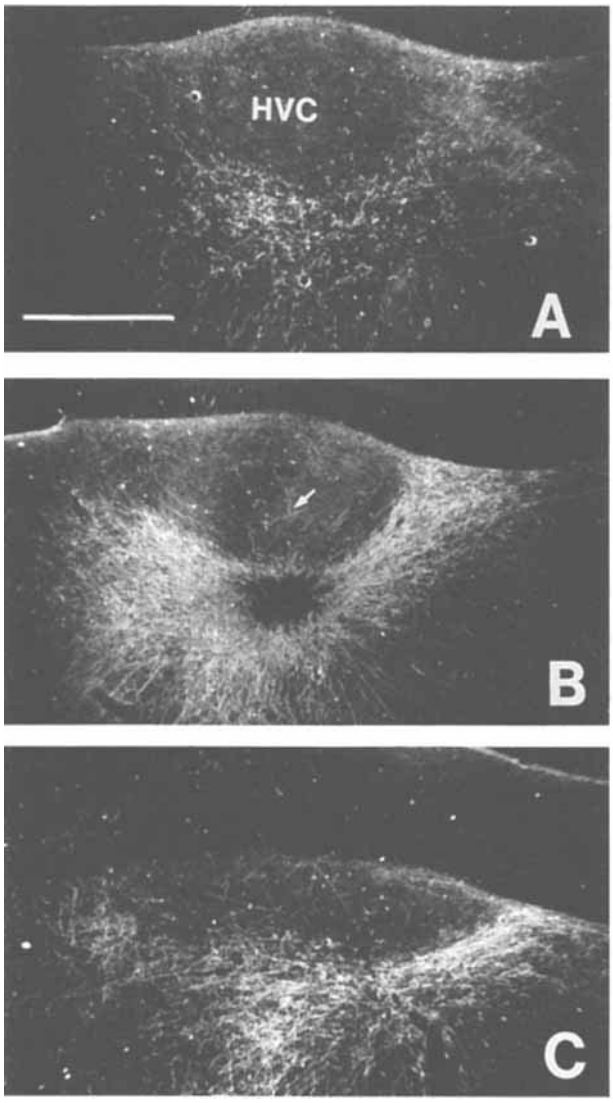

Fig. 21. **A–C:** A lateral-to-medial series of parasagittal darkfield photomicrographs (A is most lateral, C is most medial; section interval = 300 μm) of an injection of biocytin into the HVC shelf showing how labeled fibers stay within a well-defined region 300–400 μm below the ventral border of HVC. Note how the fibers run extensively within the same mediolateral plane as the injection, forming a particularly dense plexus of terminals rostral to HVC. The arrow in B indicates one fiber that penetrates into HVC. Dorsal is up, and anterior is to the right. Scale bar = 500 μm.

because they demonstrated an interesting feature of neurons along the ventral border of HVC. Many of the HVC neurons that rested on the ventral border had long, spiny dendrites extending far ventral of the HVC border into the underlying shelf (Fig. 23). A similar observation has been made with intracellular injection of tracers into physiologically identified HVC neurons (summarized by Margoliash, 1987) and has recently been documented by backfilling HVC projection neurons (Fortune and Margoliash, 1995). The efferent projections of the HVC shelf will be discussed in an upcoming report (Mello and Vates, unpublished observations).

DISCUSSION

The studies presented in this paper provide the most detailed account to date of the ascending connections of adult male zebra finch telencephalic auditory pathways. Our observations suggest important similarities and differences between songbird and nonsongbird auditory pathways that may be related to similarities and differences in auditory processing, perception, and memory formation in these different avian classes. The connectivity we have described, which is summarized in Figure 2, shows in detail the auditory thalamic input to the field L complex. We have also shown, by anatomical criteria, that Ncm, cHV (medial and lateral), caudal paleostriatum, HVC shelf, and RA cup are all components of telencephalic auditory pathways. Because of this work, we now have a better idea of Ncm's relation to the rest of the auditory projections of caudal telencephalon. In addition, we have documented points of auditory input to the song circuit that may be critical for providing the auditory feedback required for successful vocal learning.

Comparisons of auditory circuitry in songbirds and other avian species

Thalamic input to auditory telencephalon. Our experiments have shown that the primary targets of the Ov complex in the telencephalon are fields L2a and L2b, with weaker projections to L1, L3, cHV, and Ncm. This agrees with earlier observations on the projections of the Ov complex in pigeons (Karten, 1967), guinea fowl (Bonke et al., 1979a), and canaries (Kelley and Nottebohm, 1979) as well as with more recent reports on avian auditory connections in budgerigars (Brauth et al., 1987, 1994), ring doves (Durand et al., 1992), and pigeons (Wild et al., 1993). From our results, we have concluded that the Ov complex of zebra finches consists of at least three parts: 1) the Ov core, which projects predominantly to field L2a; 2) a ventromedial subregion within the core that we have identified as Ovm (following the preliminary observations of Fortune and Margoliash, 1991), which projects to field L2b; and 3) the Ov shell, a layer of neurons surrounding, and perhaps overlapping with the outer reaches of the core, that project predominantly to fields L1 and L3, to Ncm, and to clHV.

Durand et al. (1992) and Wild et al. (1993) have drawn similar conclusions about Ov projections in ring doves and pigeons, respectively, with only minor differences. Wild et al. (1993) identified a separate nucleus, the semilunaris parovoidalis (SPO), as the source of input to field L2b. Because earlier work by Wild (1987) showed that SPO receives lemniscal afferents in pigeons, the homology between Ovm in zebra finches and SPO in pigeons may be resolved most easily by determining whether Ovm or any other part of the Ov complex receives input from the lateral lemniscus. Durand et al. (1992) described the Ov shell in ring doves as also projecting to caudomedial hypothalamic structures presumably involved in regulation of endocrine function, thereby providing a link between the auditory and endocrine systems necessary for endocrine-mediated behavior in ring doves (Lehrman and Friedman, 1969; Nottebohm and Nottebohm, 1971; Cheng, 1986). A similar, as yet undescribed connection could serve to link vocal communication in songbirds to aspects of endocrine function that are influenced by auditory stimulation (Kroodsma, 1976). However, the Ov shell we identified in zebra finches and the

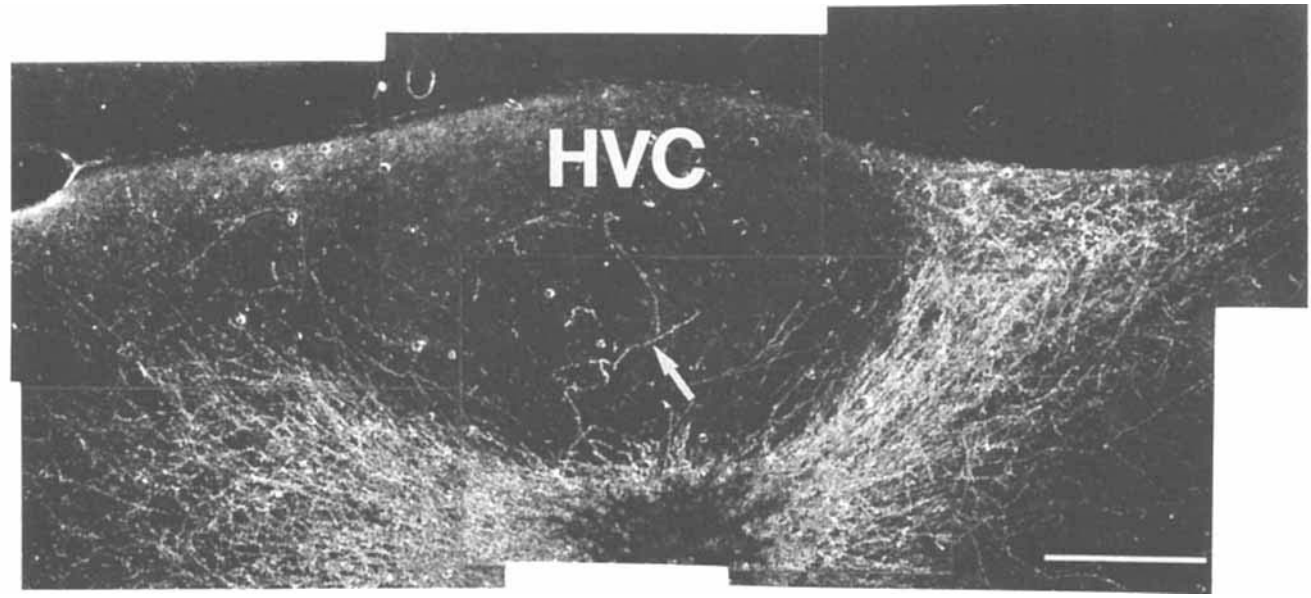

Fig. 22. A higher magnification photomicrograph montage of the same parasagittal section shown in Figure 21B. This biocytin injection, although it is located immediately below the ventral border of HVC, respects the limits of HVC, with no leakage above the shelf. The arrow marks the same fiber indicated in Figure 21B; it can be seen that this is one of only a few fibers that penetrate into the body of HVC. Dorsal is up, and anterior is to the right. Scale bar = 200 μm.

shell Durand et al. (1992) identified in ring doves may be significantly different. We identified the shell as cells in the Ov periphery and tOv that are confined by the myelinated fiber capsule around Ov and tOv and that were backfilled by injections of retrograde tracers into different parts of the field L complex. In contrast, Durand et al. (1992) identified the shell as collections of cells located medial, lateral, anterior, and posterior to the central core of cells in Ov, but separated at most points from the central core by fibrous laminae, which were labeled by injections of retrograde tracers into portions of the caudomedial hypothalamus and the caudal paleostriatum. Nonetheless, the results of the work of Durand et al. (1992) and our results coincide in an important point: the Ov shell in both ring doves and zebra finches appears to project specifically to parts of the field L complex outside of field L2a as well as to cHV and Ncm. Whether or not the Ov shell plays a role in the ontogeny of learned vocalizations, it seems to be conserved between learners and nonlearners.

Intratelencephalic connections in auditory pathways. Our data indicate that fields L2a and L2b act as the principal point of access for auditory information entering caudal telencephalon from the Ov core in zebra finches. Fields L2a and L2b then relay this information to fields L1 and L3 and to clHV, from which the information is distributed in a complex network involving cmHV, Ncm, caudal paleostriatum, HVC shelf, and RA cup. In some of these areas, the information from the Ov core may converge with a different channel of auditory input originating in the Ov shell, whose function is not presently known. The concept of a serial progression of auditory processing centers, starting in fields L2a and L2b and fanning outward into adjacent auditory neostriatum, has been proposed based on physiological and anatomical data from a variety of species (Saini and Leppelsack, 1981; Brauth et al., 1987, 1994; Brauth and McHale, 1988; Heil and Scheich, 1991b; Durand et al., 1992; Wild et al., 1993). Now, our work in zebra finches has provided a pattern of connectivity between these regions that supports this concept of serial processing in the auditory system. However, our work and that of others have added the possibility of parallel streams (in the case of zebra finches, from the Ov shell) that converge with the serial stream at particular points in the auditory pathway. At present, the purpose of such a convergence is unknown in songbirds. A third ascending auditory pathway has been described in budgerigars, and this pathway may be the primary source of auditory cues for vocal learning in budgerigars (Brauth et al., 1994); however, this latter pathway, which may or may not occur in songbirds, is distinct from the circuits we describe involving Ov core and Ov shell.

Of particular interest in these previous studies is the observation that, in nonsongbirds (i.e., guinea fowl, budgerigars, and pigeons), parts of the field L complex project to the dorsal neostriatum, which we believe is homologous to the HVC shelf in songbirds (Bonke et al., 1979a; Brauth and McHale, 1988; Wild et al., 1993; Brauth et al., 1994). This suggests that this projection is phylogenetically old and that perhaps the function of a shelf area in dorsal neostriatum is common to songbird and nonsongbird species. This case will be argued more fully in an upcoming report that will include a more complete account of efferent projections from the shelf (Mello et al., in preparation).

Although there is an overall similarity between the auditory pathways of zebra finches and Columbiformes, the connections in zebra finches include many more points of bidirectional flow of information. For instance, Wild et al. (1993) did not report any connections between fields L1 and L3 in pigeons; but, in the zebra finch, these two auditory centers are intimately interconnected. Wild et al. (1993)

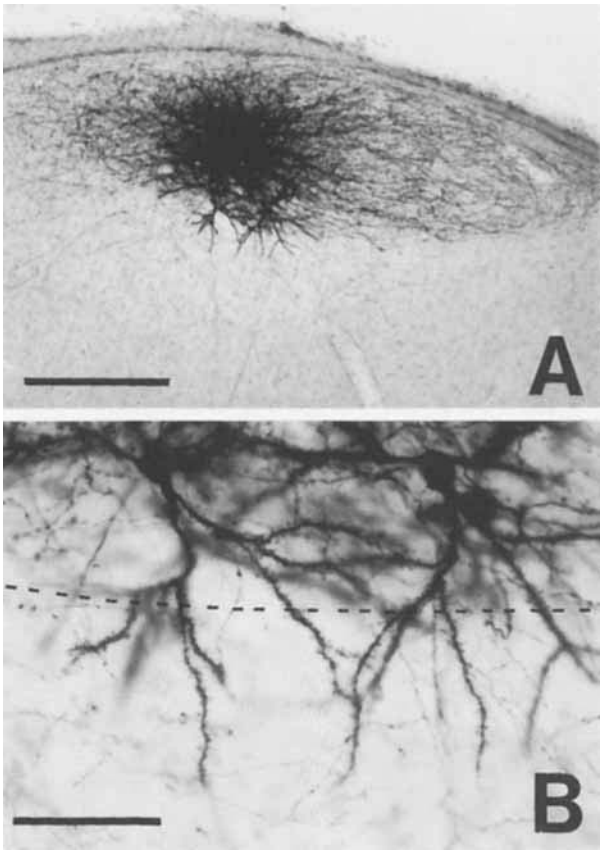

Fig. 23. **A:** An injection of biocytin into HVC that labels a small number of cells on the ventral border of HVC, whose dendrites extend into the shelf. Note how this small injection, which fills only a small percentage of the total volume of HVC, also labels fibers that run throughout all of HVC. **B:** Higher magnification view of the ventral HVC border near the injection site showing neurons along the ventral HVC border with spiny dendrites dangling into the shelf. The ventral border of HVC is indicated by the dashed line. Scale bars = 200 μm in A, 100 μm in B.

only documented that HV projects to field L2a in pigeons; in contrast, we observed rich projections connecting clHV reciprocally to several parts of the field L complex, as well as reciprocal connections between cmHV and Ncm. Also, Wild et al. (1993) showed no connection between portions of field L and the ventromedial and dorsomedial nuclei of the intermediate archistriatum (Aivm and Aidm, respectively). We believe that these archistriatal nuclei are analogous to the cup of archistriatal tissue rostral to the RA of songbirds (Mello and Vates, unpublished observations), but in contrast to Wild et al. (1993), we observed strong input to the cup from fields L1 and L3. We have confirmed many of these connections in canaries (e.g., projections of Ov core and shell, projections of fields L1 and L3 to shelf and cup), and they seem to be true of at least two songbird species (Vates, unpublished observations). Of course, these differences in connectivity between oscine songbirds and Columbiformes may result from idiosyncrasies of uptake and transport of the various compounds used for pathway tracing in different species and in different laboratories, but we believe that they may reflect evolutionary changes associated with vocal learning. This conclusion has been corroborated by studies in budgerigars, which have evolved separately from oscine songbirds, yet, like songbirds, they are capable of vocal imitation (Dooling et al., 1987; Heaton and Dooling, 1993; Farabaugh et al., 1994) and also have much more complex auditory circuits than pigeons (Brauth et al., 1994).

Caudal paleostriatum. Previous reports have suggested that caudal paleostriatum, specifically PA and PP, receives auditory input (Bonke et al., 1979a; Durand et al., 1992; Wild et al., 1993). In particular, Durand et al. (1992) showed that Ov core and shell send direct projections to PA and PP in ring doves, and Wild et al. (1993) showed that PA receives input from the Ov complex in pigeons. Our anterograde injections suggested that caudal paleostriatum is indeed an auditory target, receiving input from fields L1, L2b, and L3 in addition to possible input from Ov and L2a. However, we did not attempt to confirm these projections retrogradely. Although the projections from the caudal paleostriatum are unknown, this area may well serve an as yet unexplored role in auditory processing and memory formation, as indicated by studies in budgerigars that identified the ventral paleostriatum as an essential center for vocal learning in that species (Brauth et al., 1994).

Auditory connections of the zebra finch Ncm and cmHV

Our results have established links between Ncm, cmHV, and forebrain auditory pathways in songbirds and are consistent with results of electrophysiology and gene expression studies showing that auditory input is processed in Ncm and cmHV. Because no similar electrophysiologic or gene expression studies have been performed in nonsongbirds, we cannot formulate comparisons to nonsongbird species. Clearly, however, the interconnectivity of all of these auditory target areas suggests that auditory processing involves extensive areas of the caudal telencephalon in zebra finches, such that serial and parallel pathways may exist that process various aspects of auditory information. Because long-term habituation in Ncm is selective to conspecific sounds (Chew et al., 1995a,b), this part of the auditory circuit may play an important role both in the recognition of conspecific signals and in the formation of long-term memories of those signals. A role for Ncm in the formation of perceptual memories has been supported further by work in canaries showing the enhanced expression of ZENK in Ncm after training in an auditory operant conditioning task and interference with this task by lesions of Ncm (Jarvis, 1995; Jarvis et al., 1995). We believe that the connections between Ncm, cmHV, and clHV may act as a conduit by which auditory responses originating in Ncm can then be passed back to parts of the field L complex, to the HVC shelf, and to NIf and HVC. These pathways may serve to convey conspecific song memories formed in Ncm to the vocal motor centers that might use these memories to guide song learning and vocal exchanges.

Ncm and cmHV, as shown above, receive input from the Ov shell that may represent a component of the ascending auditory system distinct from the pathway that utilizes the Ov core. Ncm also receives input from field L3, medial field L2a, and cmHV. Interestingly, labeled fibers from the Ov complex and medial field L2a covered only the rostral extent of Ncm, suggesting an anatomical difference between rostral and caudal Ncm. Data from this laboratory (Chew et al., 1995a) have suggested a possible physiological

correlate of this anatomical subdivision; although most neurons in caudal Ncm show marked habituation to repeated presentation of a conspecific song, rostral Ncm neurons do not habituate, but continue responding vigorously. In addition, evoked auditory responses in rostral Ncm are more brisk than in caudal Ncm, with a shorter latency (Chew, personal communication); this is consistent with our observation that rostral Ncm receives direct input from the auditory thalamus and medial L2a, which it may then relay to caudal Ncm. It is important to note, however, that we have made no attempt yet to correlate specific physiological recording sites with boundaries in Ncm revealed by tracer injections into medial L2a or Ov within the same brain. Therefore, the link between anatomical and physiological landmarks is suggestive, but it is not proven.

Connections between auditory and vocal motor pathways of caudal telencephalon

The shelf of neostriatum under HVC is one of the main targets for axons originating from parts of the field L complex and clHV. It is important to note that not one of the terminal fields identified by our injections was limited to the region previously described as the shelf (Kelley and Nottebohm, 1979; Nottebohm et al., 1982; Fortune and Margoliash, 1995). We believe that our differences with these original reports are due to two factors. First, the description of the shelf proposed by Nottebohm et al. (1982) and subsequently supported by Fortune and Margoliash (1995) was based on a very conservative cytoarchitectonic boundary observed in Nissl-stained sections and is unrelated to anatomical connections of the neostriatum immediately underneath HVC. Second, the definition of the shelf in Kelley and Nottebohm (1979) was based on tract-tracing methods (tritiated amino acids), which are inferior in terms of sensitivity and specificity to the methods used in the present report. For instance, Kelley and Nottebohm (1979) stated that tracers were injected into what was then described as "field L"; we believe that this would now correspond to field L2a in our terminology, yet our experiments showed no projection from L2a to the shelf. We conclude, therefore, that the results described in Kelley and Nottebohm (1979) identified only a subset of the projection from field L1 and L3 to shelf due to partial spread of the tracer into these areas from L2a. Our conclusion has been supported by our reexamination of the material from those experiments.

The reality of the HVC shelf, as described in the present report, is emphasized by the rich plexus of connections within the shelf that run in the parasagittal plane, parallel to the ventral border of HVC. By contrast, we saw little interconnectivity with regions of neostriatum immediately ventral to the shelf (e.g., field L2b), suggesting that the shelf under HVC is distinct from deeper neostriatum. Therefore, we propose that the term shelf defines a region extending no more than 500 μm below the ventral border of HVC that receives input from fields L1 and L3 and from clHV. Because different shelf areas receive different inputs, it seems likely that not all of the shelf tissue has the same function. Taken together, these data suggest that, although the shelf is a concrete anatomical entity, it is also a complex, heterogeneous region, where the representation of different acoustic features may be anatomically segregated.

The cup of archistriatal tissue rostral to RA, like HVC and shelf, is an interesting site of apposition between an auditory center and a vocal-control nucleus. The cup receives input from fields L1 and L3 and from clHV, which essentially defines an area of archistriatum rostrodorsal to RA. Similar to the shelf, the cup has no obvious cytoarchitectonic boundary defining its outer reaches. However, the area delineated by tract-tracing studies matched well the original description of the cup (Kelley and Nottebohm, 1979). A more complete definition of the cup, its relationship with RA, and its possible role in auditory processing will be explored further in an upcoming report (Mello and Vates, unpublished observations).

Recently, Fortune and Margoliash (1995) claimed that HVC receives a direct projection from parts of the field L complex. We feel that their conclusion is premature for the following reasons. Fortune and Margoliash (1995) observed that the number of cells backfilled in field L after pressure injections of BDA into HVC was quite small, but that pressure injections of fluorescently labeled dextran amines into HVC backfilled many more cells. Our iontophoretic injections of BDA were consistently limited to HVC and, likewise, backfilled only a small number of neurons in the field L complex. We cannot rule out the possibility that these few cells projected to HVC. However, our injections into the field L complex demonstrated that fields L1 and L3, but not L2a, projected heavily to the shelf under HVC; in contrast, HVC received few axons from any part of the field L complex, and most labeled axons appeared to be on their way to the shelf. Thus, we consider it more likely that the few cells in field L backfilled after BDA injections into HVC picked up tracer through disrupted fibers of passage. With regard to data presented by Fortune and Margoliash (1995) using fluorescent dextran amines, we have found that judging the boundaries of HVC and the extent of tracer spread outside of HVC in fluorescent material is difficult; indeed, their example of a fluorescent tracer injection limited to HVC (Fortune and Margoliash, 1995; Fig. 18), suggests to us that some of their tracer leaked into rostral shelf, which would explain the much higher number of retrogradely labeled cells in field L. Fortune and Margoliash (1995) also presented injections of anterograde tracers into field L; after large pressure injections of BDA in the general area of the field L complex, they observed many anterogradely labeled fibers in HVC and only a few fibers in the shelf (see Fortune and Margoliash, 1995; Fig. 23). However, the injection they showed appears to have been centered on field L2a, which does not project to the shelf, and on the adjacent NIf, which is a known afferent to HVC. This targeting would explain why they saw very few labeled fibers in the shelf, many fibers in HVC itself, and backfilled cells in Uva, which is a previously documented afferent to NIf. Alternatively, cells in Uva could have been backfilled if these injections into the field L complex disrupted the fibers projecting from Uva to HVC as they pass through the field L complex. Finally, the injections into field L shown by Fortune and Margoliash (1995) also backfilled cells in HVC. These cells (presumably HVC cells that projected to area X) may have had axon collaterals within HVC. In sum, we believe that a direct projection from the field L complex to HVC remains unproven. The definitive proof of such a projection, if it exists, will require intracellular labeling of individual cells.

Our experiments have detailed two pathways for conveying auditory information to the vocal motor circuit, although more may exist. First, it appears that HVC and shelf are interconnected. We observed cells along the ventral border of HVC with spiny dendrites extending far into the

shelf below. Such cells are well placed to "listen" to the auditory information coursing through the dorsal layer of the shelf. Preliminary observations by Katz from intracellular injections into HVC of Lucifer yellow (summarized in Margoliash, 1987) showed similar cells on the ventral border of HVC with axons that branched widely within HVC. In addition, a recent report by Fortune and Margoliash (1995) showed two examples of RA-projecting and X-projecting cells along the ventral border of HVC that extended their dendrites into the shelf. Thus, HVC appears to contain a ventral layer of cells that conveys auditory information from the shelf to the rest of the cells within HVC. Margoliash (1983) reported that, in white-crowned sparrows, units that responded selectively to playbacks of conspecific song occurred mainly within the dorsal half of HVC, whereas tone burst-responsive units were more common within the ventral half of HVC. Although the author described these data as anecdotal and subject to collection bias, they are consistent with the proposition that auditory information filters into HVC through its ventral border and then is further distilled and integrated as it percolates up through local interconnections within HVC into the more dorsal parts of this song center. In addition, our data show that some cells in the shelf project to HVC. This is in agreement with Katz and Gurney (1981), whose intracellular injections of horseradish peroxidase into shelf neurons showed a projection from shelf to HVC. These axons could carry the auditory signals processed within the shelf to HVC, but in our material their number was disappointingly small, and more recent work by Katz (summarized by Margoliash, 1987) indicates that intracellular injection of Lucifer yellow into shelf neurons revealed very few axons penetrating into HVC proper, and most of those axons appeared to be passing fibers.

A second point of access for auditory information into the motor circuit is NIf. Our studies showed that NIf receives a projection from clHV. In addition, our experiments showed that clHV is well connected to all parts of the field L complex, and studies in starlings have recorded robust auditory responses in this area (Müller and Leppelsack, 1985). NIf also has strong auditory responses (Williams, 1989, personal communication), although their specificity and complexity have yet to be well characterized. NIf is known to project to HVC, and lesions of NIf disrupt normal song production in zebra finches (McCasland and Konishi, 1981; McCasland, 1987), although its role in vocal development is unknown. Our discovery of a connection between clHV and NIf raises the possibility that this part of the song circuit provides auditory-motor interactions essential for song learning.

It is interesting that the possible sources of auditory input to the song circuit listed above are all far along the auditory integration chain and converge on HVC. This has two implications. First, it suggests that HVC should show relatively long latencies to auditory stimuli, because it receives auditory cues that have passed across many synapses. Second, it implies that the auditory input received by HVC is already a highly distilled product. Both of these conclusions are supported by previous work which, while performed in a number of different songbird species under different conditions of anesthesia and stimulation, showed that HVC has very complex auditory responses that are often tuned maximally to the bird's own song (Margoliash, 1983, 1986; Margoliash and Fortune, 1992; Sutter and Margoliash, 1994), with latencies of approximately 18–25 msec (Margoliash, 1983; Williams, 1989; Sutter and Margoliash, 1994; Vates, personal observations) compared to 8 msec in field L2a (Williams, 1989; Vates, personal observations).

As a final note on the relationship between auditory and vocal motor pathways, it is important to remember that there is a set of more anterior telencephalic circuits involving area X, the medial nucleus of the dorsolateral thalamus (DLM), and the lateral magnocellular nucleus of the anterior neostriatum (lMAN) that are not necessary for song production but without which vocal learning cannot occur (Bottjer et al., 1984, 1989; Williams, 1989; Sohrabji et al., 1990; Scharff and Nottebohm, 1991; Doupe and Konishi, 1991; Vicario and Yohay, 1993; Vates and Nottebohm, 1995; Johnson et al., 1995). All of these nuclei have been shown to have strong auditory responses (Williams, 1989), with preference given to the bird's own song (Doupe and Konishi, 1991). Our experiments failed to reveal any connections between the anterior forebrain pathway and the auditory circuit; thus, in the absence of other evidence, we infer that auditory signals in these anterior nuclei originate in the projection from HVC to area X. This conclusion is supported by the relative latencies of auditory responses at various points in this pathway (Williams, 1989).

CONCLUSIONS

Our study constitutes the most detailed description yet of ascending auditory connections in the caudal telencephalon of an oscine songbird. Many of the pathways we have described have obvious homologies in other nonsongbird groups. However, we have been struck by the fact that the web of auditory connections we have described in adult male zebra finches is more complex and includes more reciprocal connections than that seen in nonsong-learning species (e.g., pigeon). We have proposed that some of this complexity is related to the fact that vocal ontogeny in songbirds is guided by auditory feedback. We have also shown that Ncm and cmHV, which give strong genomic and physiologic responses to playbacks of conspecific song, are far along the auditory processing chain in caudal telencephalon and, moreover, are linked by mutual interconnections. Finally, we have described two places in the song system, HVC and NIf, that may act as points of entry for auditory information. These two bridges may play a particularly important role in the auditory-guided vocal ontogeny of zebra finches.

ACKNOWLEDGMENTS

We thank David Vicario for his critical reading and very helpful comments on this paper. We also thank Daun Jackson, Sharon Sepe, and Helen Ecklund for their attentive birdkeeping. This work was supported by Public Health Service grant MH18343 to F.N. and by National Institutes of Health grant GM07739 to G.E.V.

LITERATURE CITED

Alvarez-Buylla, A., and D.S. Vicario (1988) Simple microcomputer system for mapping tissue sections with the light microscope. J. Neurosci. Methods *25:*165–173.

Beecher, M.D., M.B. Medvin, P.K. Stoddard, and P. Loesche (1986) Acoustic adaptations for parent-offspring recognition in swallows. Exp. Biol. *45:*179–193.

Bonke, B.A., D. Bonke, and H. Scheich (1979a) Connectivity of the auditory forebrain nuclei in the guinea fowl (*Numida meleagris*). Cell Tissue Res. *200:*101–121.

Bonke, D., H. Scheich, and G. Langer (1979b) Responsiveness of units in the auditory neostriatum of the guinea fowl (*Numida meleagris*) to species-specific calls and synthetic stimuli. I. Tonotopy and functional zones of field L. J. Comp. Physiol. *132:*243–255.

Bottjer, S.W., E.A. Miesner, and A.P. Arnold (1984) Forebrain lesions disrupt development but not maintenance of song in passerine birds. Science *224:*901–903.

Bottjer, S.W., K.A. Halsema, S.A. Brown, and E.A. Miesner (1989) Axonal connections of a forebrain nucleus involved with vocal learning in zebra finches. J. Comp. Neurol. *279:*312–326.

Brauth, S.E., and C.M. McHale (1988) Auditory pathways in the budgerigar II. Intratelencephalic pathways. Brain Behav. Evol. *32:*193–207.

Brauth, S.E., C.M. McHale, C.A. Brasher, and R.J. Dooling (1987) Auditory pathways in the budgerigar I. Thalamo-telencephalic projection. Brain Behav. Evol. *30:*174–199.

Brauth, S.E., J.T. Heaton, S.E. Durand, W. Liang, and W.S. Hall (1994) Functional anatomy of forebrain auditory pathways in the budgerigar (*Melopsittacus undulatus*). Brain Behav. Evol. *44:*210–233.

Brenowitz, E. (1991) Altered perception of species-specific song by female birds after lesions of a forebrain nucleus. Science *251:*303–305.

Brenowitz, E.A., and A.P. Arnold (1989) Accumulation of estrogen in a vocal control brain regions of a duetting song bird. Brain Res. *480:*119–125.

Brooks, R.J., and J.B. Falls (1975) Individual recognition by song in white-throated sparrow. III. Song features used in individual recognition. Can. J. Zool. *53:*1749–1761.

Cheng, M.F. (1986) Individual behavioral response mediates endocrine changes induced by social interaction. Ann. NY Acad. Sci. *474:*4–12.

Chew, S.J., C.V. Mello, F. Nottebohm, E. Jarvis, and D.S. Vicario (1995a) Decrements in auditory responses to a repeated conspecific song are long-lasting and require two periods of protein synthesis in the songbird forebrain. Proc. Natl. Acad. Sci. USA *92:*3406–3410.

Chew, S.J., D.S. Vicario, and F. Nottebohm (1995b) A large capacity memory system that recognized the calls and songs of individual birds. Proc. Natl. Acad. Sci. USA (in press).

Cynx, J., H. Williams, and F. Nottebohm (1992) Hemispheric differences in avian song discrimination. Proc. Natl. Acad. Sci. USA *89:*1372–1375.

Dooling, R.J., B.F. Gephart, P.H. Price, C. McHale, and S.E. Brauth (1987) Effects of deafening on the contact call of the budgerigar (*Melopsittacus undulatus*). Anim. Behav. *35:*1264–1266.

Doupe, A.J., and M. Konishi (1991) Song-selective auditory circuits in the vocal control system of the zebra finch. Proc. Natl. Acad. Sci. USA *88:*11339–11343.

Durand, S.E., J.M. Tepper, and M.-F. Cheng (1992) The shell region of the nucleus ovoidalis: A subdivision of the avian auditory thalamus. J. Comp. Neurol. *323:*495–518.

Falls, J.B. (1982) Individual recognition by sounds in birds. In Kroodsma, D.E., E.H. Miller, and H. Ouellet (eds): Acoustic Communication in Birds. New York: Academic Press, pp. 237–278.

Falls, J.B., J.R. Krebs, and P.K. McGregor (1982) Song matching in the great tit (*Parus major*): The effect of similarity and familiarity. Anim. Behav. *30:*997–1009.

Falls, J.B., A.G. Horn, and T.E. Dickson (1988) How western meadowlarks classify their songs: Evidence from song matching. Anim. Behav. *36:*579–585.

Farabaugh, S.M., A. Linzenbold, and R.J. Dooling (1994) Vocal plasticity in budgerigars (*Melopsittacus undulatus*): Evidence for social factors in the learning of contact calls. J. Comp. Psychol. *108:*81–92.

Fortune, E.S., and D. Margoliash (1991) Thalamic input and cytoarchitecture of auditory neostriatum in zebra finch. Soc. Neurosci. Abstr. *17:*446.

Fortune, E.S., and D. Margoliash (1992) Cytoarchitectonic organization and morphology of cells of the field L complex in male zebra finches (*Taenopygia guttata*). J. Comp. Neurol. *325:*388–404.

Fortune, E.S., and D. Margoliash (1995) Parallel pathways and convergence onto HVc and adjacent neostriatum of adult zebra finches (*Taeniopygia guttata*). J. Comp. Neurol. *360:*413–441.

Godard, R. (1991) Long-term memory of individual neighbours in a migratory songbird. Nature *350:*228–229.

Hauesler, U.H.L. (1988) Topography of the thalamotelencephalic projection in the auditory system of a songbird (*Sturnus vulgaris*). In J. Syka and R.B. Masterton (eds): Auditory Pathway, Structure and Function. New York: Plenum Press, pp. 197–202.

Heaton, J.T., and R.J. Dooling (1993) Effect of deafening on the contact call of adult budgerigars. Soc. Neurosci. Abstr. *19:*1015.

Heil, P., and H. Scheich (1991a) Functional organization of the avian auditory cortex analogue. I. Topographic representation of isointensity bandwidth. Brain Res. *539:*110–120.

Heil, P., and H. Scheich (1991b) Functional organization of the avian auditory cortex analogue. II. Topographic distribution of latency. Brain Res. *539:*121–125.

Hinde, R.A. (1958) Alternative motor patterns in chaffinch song. Anim. Behav. *6:*211–218.

Immelman, K. (1969) Song development in the zebra finch and other estrildid finches. In R.A. Hinde (ed): Bird Vocalizations. New York: Cambridge University Press, pp. 61–80.

Jarvis, E.D. (1995) A window into the molecular biology of song associative learning and memory in songbirds. Doctoral Dissertation, The Rockefeller University, New York, NY.

Jarvis, E.D., C.M. Mello, and F. Nottebohm (1995) Stimulus and behavior variables that influence the song-induced expression of an immediate early gene in the canary forebrain. Learning Mem *2:*62–80.

Johnson, F., M.M. Sablan, and S.W. Bottjer (1995) Topographic organization of a forebrain pathway involved with vocal learning in zebra finches. J. Comp. Neurol. *358:*260–278.

Karten, J.H. (1967) The organization of the ascending auditory pathway in the pigeon (*Columba livia*) I. Diencephalic projection of the inferior colliculus (nucleus mesencephali lateralis, pars dorsalis). Brain Res. *6:*409–427.

Karten, J.H. (1968) The ascending auditory pathway in the pigeon (*Columba livia*) II. Telencephalic projections of the nucleus ovoidalis thalami. Brain Res. *11:*134–153.

Katz, L.C., and M.E. Gurney (1981) Auditory responses in zebra finch's motor system for song. Brain Res. *221:*192–197.

Kelley, D.B., and F. Nottebohm (1979) Projections of a telencephalic auditory nucleus-field L-in the canary. J. Comp. Neurol. *183:*455–470.

Konishi, M. (1965) The role of auditory feedback in the control of vocalization in the white-crowned sparrow. Z. Tierpsychol. *22:*770–783.

Krebs, J.R. (1977) The significance of song repertoire: The Beau Geste hypothesis. Anim. Behav. *25:*475–478.

Kroodsma, D.E. (1976) Reproductive development in a female songbird: Differential stimulation by quality of male song. Science *192:*574–575.

Kroodsma, D.E. (1982) Learning and the ontogeny of sound signals in birds. In Kroodsma, D.E., E.H. Miller, and H. Ouellet (eds): Acoustic Communication in Birds. New York: Academic Press, pp. 1–23.

Lehrman, D.S., and M. Friedman (1969) Auditory stimulation of ovarian activity in the ring dove (*Streptopelia risoria*). Anim. Behav. *17:*494–497.

Margoliash, D. (1983) Acoustic parameters underlying the responses of song-specific neurons in the white-crowned sparrow. J. Neurosci *3:*1039–1057.

Margoliash, D. (1986) Preference for autogenous song by auditory neurons in a song system nucleus of the white-crowned sparrow. J. Neurosci. *6:*1643–1661.

Margoliash, D. (1987) Neural plasticity in birdsong learning. In J.P. Rauschecker and P. Marler (eds): Imprinting and Cortical Plasticity. New York: John Wiley and Sons, pp. 23–54.

Margoliash, D., and E.S. Fortune (1992) Temporal and harmonic combination-sensitive neurons in the zebra finch's HVc. J. Neurosci. *12:*4309–4326.

Marler, P., and S. Peters (1977) Selective vocal learning in a sparrow. Science *198:*519–527.

Marler, P., and S. Peters (1981) Sparrows learn adult song and more from memory. Science *213:*780–782.

Marler, P., and S. Peters (1982) Long term storage of learned bird songs prior to production. Anim. Behav. *30:*479–482.

Marler, P., and M. Tamura (1964) Culturally transmitted patterns of vocal behavior in sparrows. Science *146:*1483–1486.

McCasland, J.S. (1987) Neuronal control of bird song production. J. Neurosci. *7:*23–39.

McCasland, J.S., and M. Konishi (1981) Interaction between auditory and motor activities in an avian song control nucleus. Proc. Natl. Acad. Sci. USA *78:*7815–7819.

Mello, C.V., and D.F. Clayton (1994) Song-induced ZENK gene expression in auditory pathways of songbird brain and its relation to the song control system. J. Neurosci. *14:*6652–6666.

Mello, C.V., D.S. Vicario, and D.F. Clayton (1992) Song presentation induces gene expression in the songbird forebrain. Proc. Natl. Acad. Sci. USA *89:*6818–6822.

Mello, C.V., F. Nottebohm, and D.F. Clayton (1995) Repeated exposure to one song leads to a rapid and persistent decline in an immediate early gene's response to that song in zebra finch telencephalon. J. Neurosci. *15:*6919–6925.

Müller, C.M., and H.-J. Leppelsack (1985) Feature extraction and tonotopic organization in the avian auditory forebrain. Exp. Brain Res. *59:*587–599.

Müller, C.M., and H. Scheich (1985) Functional organization of the avian auditory field L—A comparative 2dg study. J. Comp. Physiol. *156:*1–12.

Nordeen, K.W., and E.J. Nordeen (1992) Auditory feedback is necessary for the maintenance of stereotyped song in adult zebra finches. Behav. Neurol. Biol. *57:*58–66

Nottebohm, F. (1968) Auditory experience and song development in the chaffinch, *Fringilla coelebs*. Ibis *110:*549–568.

Nottebohm, F. (1972) The origins of vocal learning. Am. Nat. *106:*116–140.

Nottebohm, F., and M.E. Nottebohm (1971) Vocalizations and breeding behavior of surgically deafened ring doves (*Streptopelia risoria*). Anim. Behav. *19:*313–327.

Nottebohm, F., T.M. Stokes, and C.M. Leonard (1976) Central control of song in the canary, *Serinus canaria*. J. Comp. Neurol. *165:*457–486.

Nottebohm, F., D.B. Kelley, and J.A. Paton (1982) Connections of vocal control nuclei in the canary telencephalon. J. Comp. Neurol. *207:*344–357.

Okuhata, S., and F. Nottebohm (1992) Nucleus Uva might be a part of a feedback circuit for song processing. Soc. Neurosci. Abstr. *18:*527.

Okuhata, S., and N. Saito (1987) Synaptic connections of thalamo-cerebral vocal nuclei of the canary. Brain Res. Bull. *18:*35–44.

Peek, F.W. (1972) An experimental study of the territorial function of vocal and visual display in the male red-winged blackbird (*Agelaius phoeniceus*). Anim. Behav. *20:*112–118.

Price, P.H. (1979) Developmental determinants of structure in zebra finch song. J. Comp. Physiol. Psychol. *93:*260–277.

Rose, M. (1914) Über die cytoarchitektonische Gliederung des Vorderhirns der Vogel. J. Psychol. Neurol. *21:*278–352.

Saini, K.D., and H.J. Leppelsack (1981) Cell types of the auditory caudomedial neostriatum of the starling (*Sturnus vulgaris*). J. Comp. Neurol. *198:*209–229.

Scharff, C., and F. Nottebohm (1991) A comparative study of the behavioral deficits following lesions of various parts of the zebra finch song system: Implications for vocal learning. J. Neurosci. *11:*2896–2913.

Scheich, H. (1990) Representational geometries of telencephalic auditory maps in birds and mammals. In B.L. Finlay (ed): The Neocortex. New York: Plenum Press, pp. 119–136.

Scheich, H., B.A. Bonke, D. Bonke, and G. Langer (1979) Functional organization of some auditory nuclei in the guinea fowl demonstrated by the 2-deoxyglucose technique. Cell Tissue Res. *204:*17–27.

Simpson, H.B., and D.S. Vicario (1990) Brain pathways for learned and unlearned vocalization differ in zebra finches. J. Neurosci. *10:*1541–1556.

Sohrabji, F., E.J. Nordeen, and K.W. Nordeen (1990) Selective impairment of song learning following lesions of a forebrain nucleus in the juvenile zebra finch. Behav. Neural Biol. *53:*51–63.

Stokes, T.M., C.M. Leonard, and F. Nottebohm (1974) The telencephalon, diencephalon, and mesencephalon of the canary, *Serinus canaria*, in stereotaxic coordinates. J. Comp. Neurol. *156:*317–374.

Sutter, M.L., and D. Margoliash (1994) Global synchronous response to autogenous song in zebra finch HVc. J. Neurophysiol. *72:*2105–2123.

Thorpe, W.H. (1958) The learning of song patterns by birds, with special reference to the song of the chaffinch, *Fringilla coelebs*. Ibis *100:*535–570.

Thorpe, W.H. (1963) Antiphonal singing in birds as evidence for avian auditory reaction time. Nature *197:*774–776.

Thorpe, W.H., and M.E.W. North (1965) Origin and significance of the power of vocal imitation: With special reference to the antiphonal singing of birds. Nature *208:*219–222.

Vates, G.E., and F. Nottebohm (1995) Feedback circuitry within a song learning pathway. Proc. Natl. Acad. Sci. USA *92:*5139–5143.

Vicario, D.S. (1991) Organization of the zebra finch song control system: II. Functional organization of outputs from nucleus robustus archistriatalis. J. Comp. Neurol. *309:*486–494.

Vicario, D.S. (1993) A new brainstem pathway for vocal control in the zebra finch song system. NeuroReport *4:*983–986.

Vicario, D.S., and F. Nottebohm (1990) Organization of the zebra finch song control system: I. Representation of syringeal muscles in the hypoglossal nucleus. J. Comp. Neurol. *271:*346–354.

Vicario, D.S., and K.H. Yohay (1993) Song-selective auditory input to a forebrain vocal control nucleus in the zebra finch. J. Neurobiol. *24:*488–505.

Weeden, J.S., and J.B. Falls (1959) Differential responses of male ovenbirds to recorded songs of neighboring and more distant individuals. Auk *66:*343–351.

Wild, J.M. (1987) Nuclei of the lateral lemniscus project directly to the thalamic auditory nuclei in the pigeon. Brain Res. *408:*303–307.

Wild, J.M. (1993) Descending projection of the songbird nucleus robustus archistriatalis. J. Comp. Neurol. *338:*225–241.

Wild, J.M. (1994) The auditory-vocal-respiratory axis in birds. Brain Behav. Evol. *44:*192–209.

Wild, J.M., H.J. Karten, and B.J. Frost (1993) Connections of the auditory forebrain in the pigeon (*Columba livia*). J. Comp. Neurol. *337:*32–62.

Wiley, R.H., and M.S. Wiley (1977) Recognition of neighbors' duets by stripe-backed wrens *Campylorhynchus nuchalis*. Behaviour *62:*10–34.

Williams, H. (1989) Multiple representations and auditory-motor interactions in the avian song system. Ann. NY Acad. Sci. *563:*148–164.

Williams, H. (1990) Models for song learning in the zebra finch: Fathers or others? Anim. Behav. *39:*745–757.

Williams, H., and F. Nottebohm (1985) Auditory responses in avian vocal motor neurons: A motor theory for song perception in birds. Science *229:*279–282.

Zann, R. (1985) Ontogeny of the zebra finch distance call: I. Effects of cross-fostering to Bengalese finches. Z. Tierpsychol. *68:*1–23.